Biaxial Orientation Studies of CARILON® Polymer

University of Toledo Study

J. R. Kastelic

Project No. 62182
CARILON® Packaging Film

PRINTED: January 1993

REVIEWERS: D. S. Brath,
APPROVAL: D. S. Brath,
PARTICIPANTS: R. N. Campbell, N. E. Peck
REFERENCES: Based on work through December 1990

SHARED – Under the Research Agreement between SIRM and Shell Oil Company dated Jan. 1, 1960, as amended.

CONFIDENTIAL

Shell Development Company
A DIVISION OF SHELL OIL COMPANY

Westhollow Research Center
Houston, Texas

ABSTRACT

A long range goal of the CARILON/R/ Thermoplastic Packaging Program is to achieve clear bottles with a stretch blow molding process. These would likely have applications for carbonated beverages and other non-carbonated uses where clarity is a requirement. Attractive clarity and gloss have been demonstrated in CARILON thermoplastic cups produced with Shell's Solid Phase Pressure Forming process and we believe the deformation process in SPPF to be very similar to that imposed in stretch blow molding. Work was initiated at the University of Toledo, who are experts in stretch blow orientation, to study CARILON deformation and assist us in developing resins and a stretch blow molding process for CARILON. This report summarizes their findings and includes a copy of their detailed study.

WRC-2840

Technical Information Record WRC-2840

BIAXIAL ORIENTATION STUDIES OF CARILON/R/ POLYMER

by

John R. Kastelic

Introduction

A long range goal of the CARILON/R/ Thermoplastic Packaging Program is to achieve clear bottles with a stretch blow molding process. It is expected that mechanical properties and barriers can be enhanced as a consequence of the orientation imparted. Thus these would likely have applications for carbonated beverages and other non-carbonated uses where clarity is a requirement and enhanced properties are desirable.

Background

Attractive clarity and gloss have been demonstrated in CARILON thermoplastic cups produced with Shell's Solid Phase Pressure Forming process. We believe the deformation process in SPPF to be very similar to that imposed in stretch blow molding. It thus appears likely that CARILON polymers can be stretch blow molded if thermal conditions similar to that required for SPPF can be achieved in a bottle preform.

However, early efforts to achieve this result have not met with much success. Danforth, Campbell, Korcz and Kastelic have all tried and failed using various machines and methods. Kastelic's efforts are documented in a separate TIR. The matter is important enough from a standpoint of potential packaging market to warrant continued efforts. It seemed best to start with a more basic approach in view of the practical difficulties already experienced with machinery in the field.

Work was initiated at the Polymer Institute at the University of Toledo under a joint industry - university R&D program with partial government funding. Professors within the institute have experience at Owens Illinois during the years of PET stretch blow molded bottle development. They are experts in stretch blow orientation and offered to study CARILON deformation as a function of drawing temperature and assist us in developing resins and a stretch blow molding process for CARILON.

Several resins made at the MDU were made available to the university of Toledo. The basic properties are given in the table below. The university was supplied with both melt extruded sheet produced at WRC and with nibs.

Resin	Melting Point	LVN
89/021	232°C	1.97
89/022	232	1.66
89/045	222	1.44
89/046	223	1.50

All lab deformation studies were performed on 89/022 and 89/046. The other two resins were used in actual stretch blow molding runs at Nissei.

The university of Toledo took a broad based approach. They studied in order the following topics:

Melting and crystallization behavior.
Rheology of the CARILON melt.
Basic mechanical properties of unoriented sheet.
Tenter frame orientation of CARILON sheet.
Mechanical properties of oriented CARILON films.
Optical properties of oriented films.
IR heating characteristics of CARILON.
Injection blow molding behavior.

Their study proved to be comprehensive and successful. With their assistance we were able to make significant progress and actually run CARILON polymers on PET equipment manufactured by Nissei. Their equipment employs an inline stretch blow molding technique. Bottles were made with either round or rectangular profile and had either a 12 or a 16 oz capacity, depending on the mold installed in the stretch station. These have been widely exhibited within Shell labs. The University of Toledo Final Report, entitled "Oriented Clear Container Development" is attached. Major conclusions of their work are listed on the next page. More information on stretch blow molding and trial results are given in second TIR entitled "Stretch Blow Molding Of CARILON Polymer" by J. R. Kastelic.

John R. Kastelic

MAJOR CONCLUSIONS

Extruded sheet was successfully biaxially oriented with a TM Long Stretcher at draw ratios up to 4X by 4X for both 89/022 and 88/046 CARILON® resins.

Biaxially oriented films produced by stretching were of excellent quality and exhibited attractive clarity and gloss. Strain hardening and accompanying enhanced mechanical properties were documented.

The load-displacement curves obtained during orientation suggest a sequential orientation process is more stable and has a broader process window than for a simultaneous process. High draw rates are also recommended.

Crystallization rates of CARILON® resins are too high to allow an amorphous morphology to be attained in any realistic preform or parison for drawing or stretch blow molding. As a consequence, stretch blow molded bottles will have opaque neck threads because local orientation is not sufficient to impart clarity.

Infra red heating of CARILON® thermoplastic results in heat absorption at the surface with little penetration into the depth of the sample. Conventional reheat stretch blow equipment designed for PET is thus not likely to be useful for CARILON®. This author recommends as an alternative dielectric heating which has been used commercially with PET.

Stretch blow molded bottles were produced on a Nissei ASB 50HT injection stretch blow molding machine over a very narrow operating window using sequential activation of stretch rod and blow air. These do exhibit enhanced clarity.

A central core layer of bottle walls appears to have remained above melting during fabrication and likely did not solidify until after bottle ejection. Although the inner and outer skins are drawn and transparent, this core material is not and overall container transparency is not equal to that achieved in SPPF. Physical properties of the core are likely not equal to that achieved in the oriented skins. Thus bust and swell testing results fall short of that ultimately achievable without this unoriented central layer.

Thinner parison or even longer thermal equilibrium times might help eliminate this core layer. An alternative possibility is to co-injection mold walls of a higher melting polyketone terpolymer than used in the core. Nissei has three layer co-injection stretch blow mold capability which was developed for PET.

Melt rheology of CARILON® thermoplastic is ideal for extrusion blow molding. However, thermal degradation was noted by the U. of Toledo both during melt processing, and in reheat orientation studies and they suggest thermo-oxidative stability "will limit the usefulness of Shell resins for preparing commercial items". Stability improvements have been recently achieved.

Oriented Clear Container Development

for

Shell Chemical Company

Phase I Final Report

University of Toledo
Polymer Institute
Toledo, Ohio

Dr. S. A. Jabarin
Dr. L. F. Chang
Michael Chang
Elizabeth Lofgren
Michael Mumford
Long Fay

October 1, 1990

Table of Contents

List of Figures

List of Tables

I. Objective

Develop technology to produce oriented clear containers from "Shell Proprietary Resin", using Shell number 89022 and 89046 resins. The preferred size and shape is a wide mouth jar.

II. Introduction

The development of a clear wide mouth oriented container from a highly crystalline material such as the "Shell Proprietary Resin" is quite complex and it involves many interrelated variables. These may include basic materials characteristics, parison and container design, injection molding process optimization, parison reheating, orientation characteristics, blow molding characterization and optimization, and process modeling and simulation. This program follows a logical sequence of technical development that address the above areas.

III. Conclusions

- Shell 89022 melts and crystallizes at a higher temperature, and has more crystallinity than 89046. Both materials crystallize rapidly. The final melting temperatures, for the initial heating of ground resin, are:

Shell 89022:	236°C
Shell 89046:	227°C

- The orientation temperature for Shell Resins, in order to eliminate yield lines (neck-in) should be:

Shell 89022:	210°C or greater.
Shell 89046:	200°C or greater.

- Both Shell Resins, 89022 and 89046, show evidence of strain hardening during orientation, an important property for improved physical properties.

- The tensile properties of oriented Shell resins are improved compared to the unoriented sheet.

- In general, film clarity is increased when the sheet is oriented to a planar strain of 9 or above. Gloss is increased by orientation above a planar strain of 15.

III. Conclusions - *continued*

- Thermal Degradation while in the melt may be the limiting processing property of Shell Proprietary Resins. Shell 89022 was more susceptable to thermal degradation than Shell 89046. Degradation will limit the usefulness of the Shell resins for preparing commercial items.

- Processing of Shell resins should be at the lowest temperature possible (≈240°C) in order to minimize melt degradation.

- Bottles were made from Shell 89045 (similar to 89046) by a Nissei Injection blow molding machine. However, Shell 89045 showed signs of thermal degradation.

- During IR heating in a PET type blow molding process, most of the heat will be absorbed in the surface region and very little radiation heat will reach the interior of the parison. Modifications to the heater system and heating procedure are required.

IV. Results and Discussion

1.0 Thermal Properties of Sheet and Resin Samples

Thermal Properties of Shell proprietary materials (89022 and 89046) have been evaluated under a variety of conditions using both sheet and ground resin. This has been done to aid in establishing preliminary conditions and material limitations required for its processing and orientation. Analyses were performed using a Perkin-Elmer Differential Scanning Calorimeter (DSC-2). All determinations were done under a nitrogen atmosphere to prevent oxidative degradation during heating.

1.1 Evaluation of General Thermal Responses

Samples were heated and cooled at 10°C per minute in order to monitor their melting and crystallization behaviors and detect thermal responses resulting from processing as well as material differences. Initial heating results indicate thermal history experienced by the sample prior to analysis. Samples cooled and reheated under equivalent conditions may be compared to each other to determine inherent differences in material properties. Table I shows results obtained for proprietary materials 89022 and 89046. These materials were characterized in the forms of "as received" sheets and ground, vacuum dried resins. DSC scans obtained for sheet samples are shown in Figures 1 and 2 while those for ground resin samples are shown in Figures 3 and 4. Individual scans are labeled to show specific thermal histories.

From results shown in Table I and Figures 1 through 4 it can be seen that 89022 melts and crystallizes at higher temperatures than 89046. Results also show that both materials are sensitive to thermal experiences. Indications of sensitivity are seen as shifts in melting and crystallization temperatures as well as changes in peak shapes and in heats of melting and crystallization (ΔH) after various treatments. Of particular note are small low temperature melting endotherms seen during the initial heating of vacuum dried resin samples. These endotherms indicate melting of crystalline structures formed in response to 45°C vacuum drying conditions.

1.2 Melting Behavior as a Function of Heating Rate

Samples of "as received" sheet were heated at rates of 2.5, 10, and 20°C per minute. These results are shown in Table II and Figures 5 and 6. It can be seen that the size and distribution of melting peaks changes with changes in heating rate. As with previous results, this behavior indicates material sensitivity to thermal treatment. These results also show that material 89046 has lower temperature melting behavior and less crystallinity than 89022 under equivalent testing conditions.

1.3 Annealing Effects on Melting Behavior

Samples of "as received" sheet were annealed for 10 and 30 minutes at temperatures of 140° and 160°C. Results, which are shown in Table III and Figures 7 and 8, show that annealing causes a slight increase in crystallinity (ΔH) after 10 minutes, that is not significantly changed by longer heating times. Peak shapes are seen to change with annealing as a small lower temperature shoulder appears. The temperature of this shoulder is dependent upon the annealing temperature and increases with higher annealing temperatures. The distribution of peaks in the major melting endotherm are also seen to shift slightly with annealing as portions of the material apparently melt and recrystallize.

1.4 Crystallization Behavior as a Function of Cooling Rate

Samples of ground, vacuum dried resin were heated quickly to temperatures of 250° and 240°C for 89022 and 89046 respectively. They were then held at this temperature for 5 minutes to remove all crystallinity and cooled at rates ranging from 5° to 80°C per minute. Results showing changes in crystallization behavior as a function of cooling rate are shown in Table IV and Figures 9 and 10. As previously noted, 89022 crystallizes at a higher temperature and to a slightly greater extent than 89046. Levels of crystallinity measured for both samples (ΔH values) are seen to decrease only slightly at rapid cooling rates. This indicates that both materials crystallize very rapidly. Crystallization peaks of both materials are shifted to lower temperatures at faster cooling rates, as a result of supercooling effects commonly noted for polymer samples.

1.5 Isothermal Crystallization Behavior

Samples of ground, vacuum dried resin were heated quickly to temperatures of 250° and 240°C for 89022 and 89046, respectively, and held for 5 minutes to remove all crystallinity. They were then quickly quenched to the desired crystallization temperature. Results shown in Table V and Figures 11 and 12 indicate times required for initial, peak and final crystallization. As previously noted, 89022 crystallizes at higher temperatures than 89046.

1.6 Specific Heat Values from 50° to 250°C

Specific heat values were determined on samples of "as received" sheet according to the procedure given in the Perkin-Elmer manual. Samples were heated at 10°C per minute for increments of about 50°C. Aluminum oxide (sapphire) standard material was used for calibration. Specific heat results are shown on Table VI and in Figures 13 and 14. It can be seen that results are similar for the two materials in the non-melting ranges, with increases caused by the melting endotherm shifted as expected for each material.

TABLE I

Thermal Behavior of Shell Samples

Shell Sample	Melting, °C				Crystallization, °C			
	Ti	Tp	Tf	ΔH,cal/g	Ti	Tp	Tf	ΔH,cal/g
SHEET - AS RECEIVED								
89022								
Initial	159	226(229)	236	20	196	185	61	-15
Reheat after crystallization	72	(131)211	224	13				
89046								
Initial	157	218,223	228	18	181	167	89	-14
Reheat after crystallization	86	200	215	14				
GROUND RESIN - VACUUM DRIED @ 40°C								
89022								
	*59	75	92	1				
Initial	178	230	239	20	195	(181)177	101	-19
Reheat after crystallization	141	213	228	16				
Reheat from quench	138	218,225	233	19				
89046								
	*60	74	90	1				
Initial	159	(213)222	227	19	186	169	90	-17
Reheat after crystallization	129	203(208)	219	15				
Reheat from quench	135	210,217	224	18				

Samples heated and cooled at 10°C/minute under a nitrogen atmosphere

*additional low temperature peak resulting form drying conditions

TABLE II

Melting as a Function of Heating Rate

Shell Sheet - As received	Melting,°C Ti	Tp	Tf	ΔH,cal/g
89022				
2.5°/min.	185	226,230	234	19
10°/min.	159	226,229	236	20
20°/min.	158	227,230	241	22
89046				
2.5°/min.	186	216,222	226	16
10°/min.	157	218,223	228	18
20°/min.	148	218,222	231	19

TABLE III

Melting Behavior as a Result of Annealing Conditions

Shell Sheet - As received	Melting,°C Ti	Tp	Tf	ΔH,cal/g
89022				
Not Annealed	159	226,(229)	236	20
Annealed @ 140°C 10 min.	140	(154),227,230	235	23
Annealed @ 140°C 30 min.	143	(152),225,226	235	23
Annealed @ 160°C 10 min.	162	(171),227,231	235	22
Annealed @ 160°C 30 min.	162	(173),229	237	23
89046				
Not Annealed	157	218,223	228	18
Annealed @ 140°C 10 min.	138	(152),217,221	229	21
Annealed @ 140°C 30 min.	143	(151),217,222	229	21
Annealed @ 160°C 10 min.	160	(171),217,222	229	20
Annealed @ 160°C 30 min.	161	(172),217,222	227	21

Samples annealed at various conditions, quenched to room temperature, and reheated at 10°C/minute.

TABLE IV

Crystallization as a Function of Cooling Rate

Shell Ground Vacuum Dried Resin	Crystallization,°C Ti	Tp	Tf	ΔH,cal/g
89022				
5°/min.	202	190	114	-22
10°/min.	200	187	103	-22
20°/min.	196	182	111	-21
40°/min.	188	176	106	-20
80°/min.	180	166	56	-20
89046				
5°/min.	194	182	112	-21
10°/min.	193	178	100	-20
20°/min.	189	174	103	-19
40°/min.	183	167	105	-19
80°/min.	177	157	76	-18

89022 heated to 250°C at 320°C/minute held 5 min. and cooled at rate indicated

89046 heated to 240°C at 320°C/minute held 5 min. and cooled at rate indicated

TABLE V

Isothermal Crystallization after Cooling from the Melt

Shell Ground Vacuum Dried Resin	Isothermal Crystallization Temperature, °C	Times Required for Crystallization, min. Ti	Tp	Tf	ΔH, cal/g
89022	195	0.6	2.5	14	-16
	200	0.8	6.6	32	-16
	205	0.7	16.3	60	-15
89046	188	too fast	2.0	7	>-13
	190	0.6	2.7	19	-15
	192	0.7	3.6	20	-16
	195	0.9	8.6	60	-16

TABLE VI

Specific Heat Values, calories/gram °C

	Shell 89022 (As received sheet)			Shell 89046 (As received sheet)		
Temperature °C	Run 1	Run 2	Average	Run 1	Run 2	Average
50	.392	.424	.408	.377	.404	.391
60	.416	.427	.422	.386	.421	.404
70	.450	.444	.447	.399	.428	.414
80	.464	.467	.466	.409	.444	.427
90	.449	.480	.465	.424	.455	.440
100	.456	.527	.492	.447	.498	.473
110	.458	.533	.496	.461	.525	.493
120	.454	.521	.488	.477	.519	.498
130	.474	.517	.496	.490	.515	.503
140	.490	.541	.516	.511	.544	.528
150	.489	.580	.535	.540	.577	.559
160	.541	.636	.589	.582	.652	.617
170	.565	.616	.591	.596	.623	.610
180	.585	.645	.615	.631	.655	.643
190	.632	.711	.672	.679	.729	.704
200	.696	.767	.732	.795	.786	.791
210	.779	.871	.825	.939	1.018	.979
215	-	.911	-	1.260	1.594	1.427
218.5	-	-	-	-	2.124	-
220	.951	1.086	1.019	1.790	1.896	1.843
225	1.486	1.577	1.532	1.030	1.051	1.041
230	2.331	>2.4	-	.548	.614	.581
235	-	.616	-	-	.564	-
240	.523	.587	.555	.559	.559	.559
250	.526	.598	.562	.595	.569	.582

Initial Melting

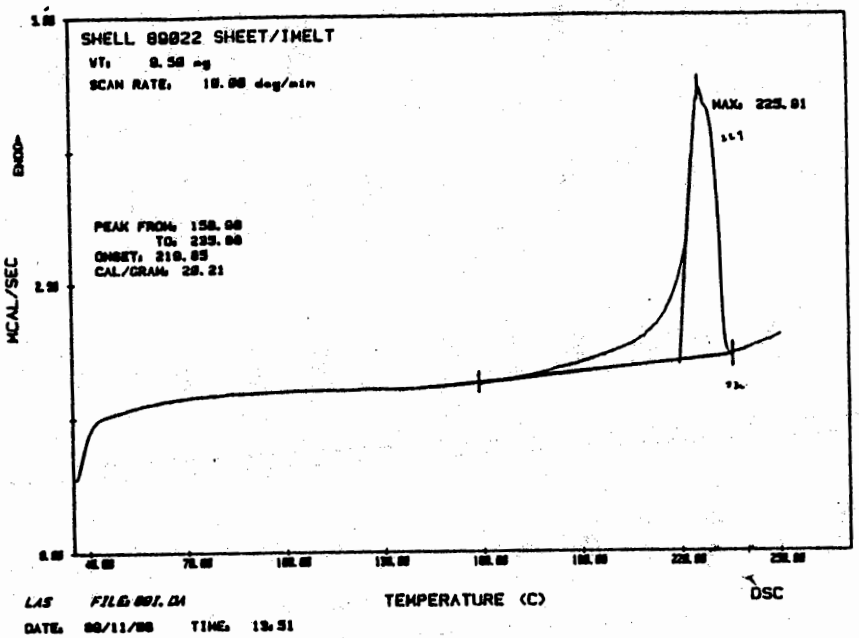

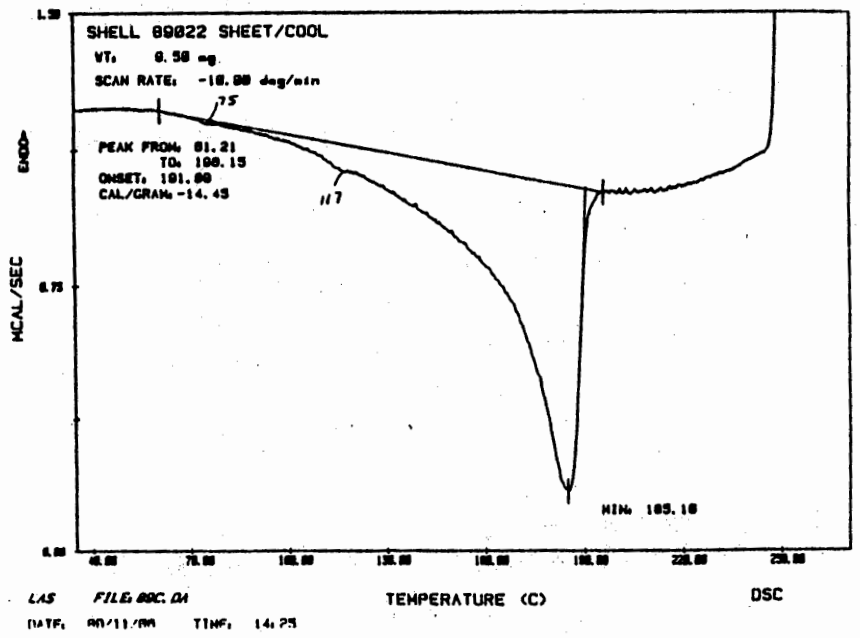

Crystallization

Shell 89022
(Sheet - As Received)

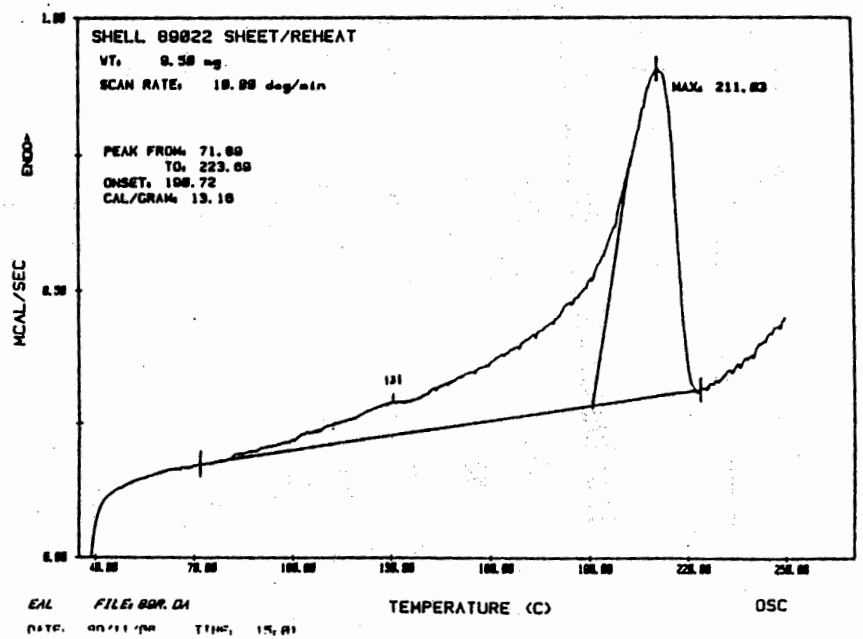

Reheat after 10°/Min. Crystallization

Fig. 1

Initial Melting

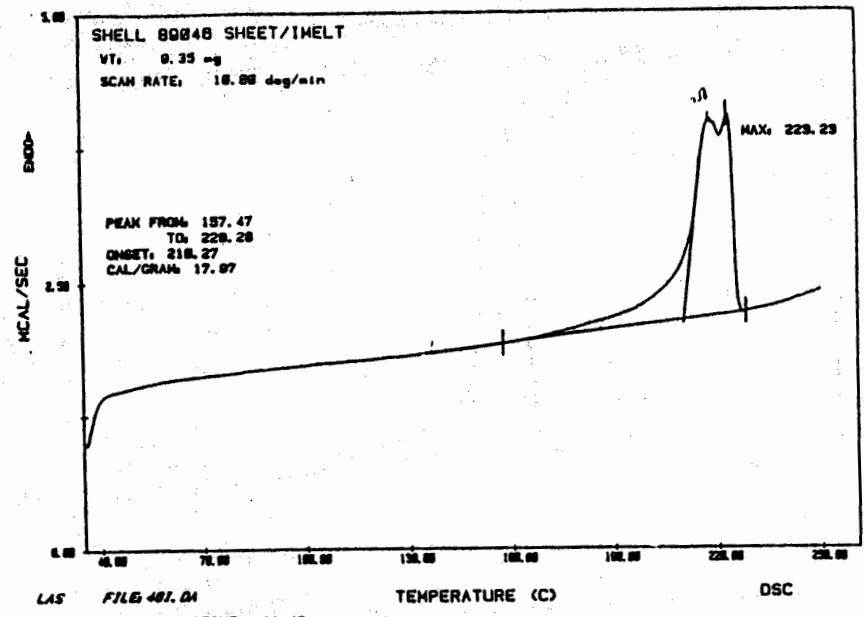

Shell 89046
(Sheet - As Received)

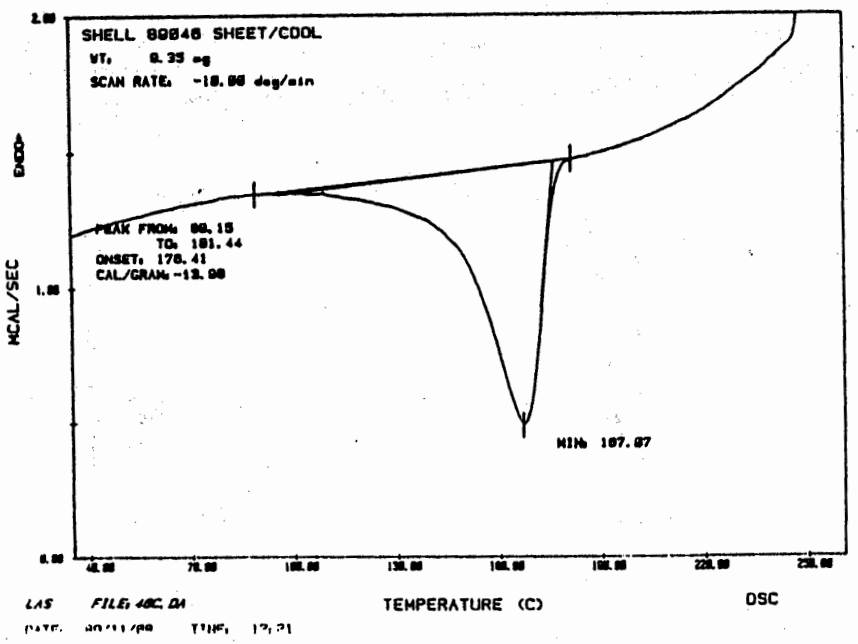

Crystallization

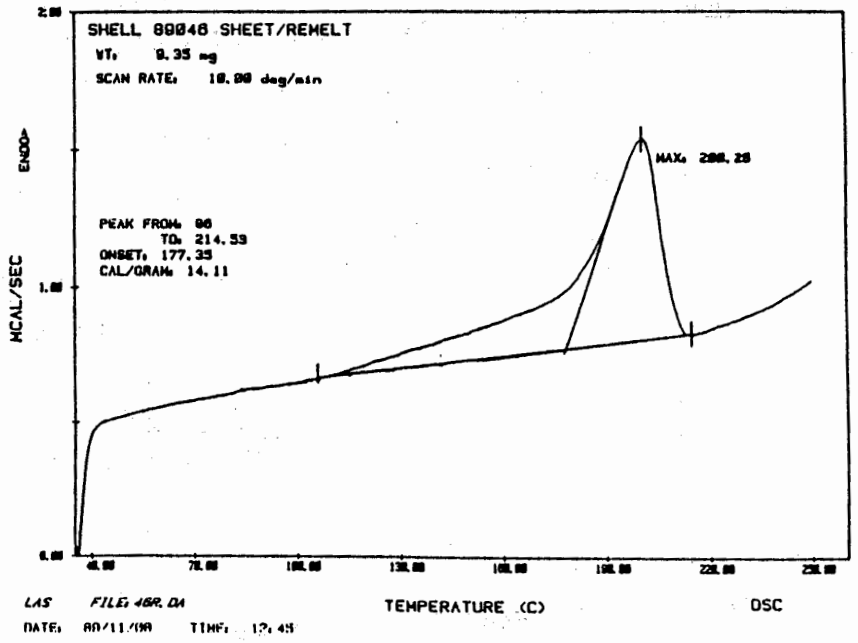

Reheat after 10°/Min. Crystallization

Fig. 2

Sl. 89022
(Ground Resin)

Initial Melting

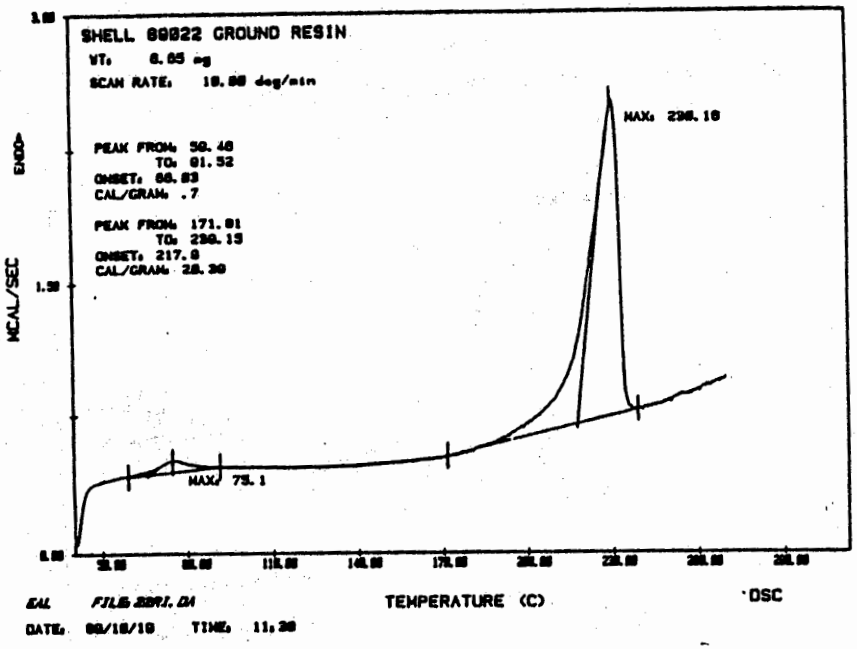

Reheat after 10°/Min. Crystallization

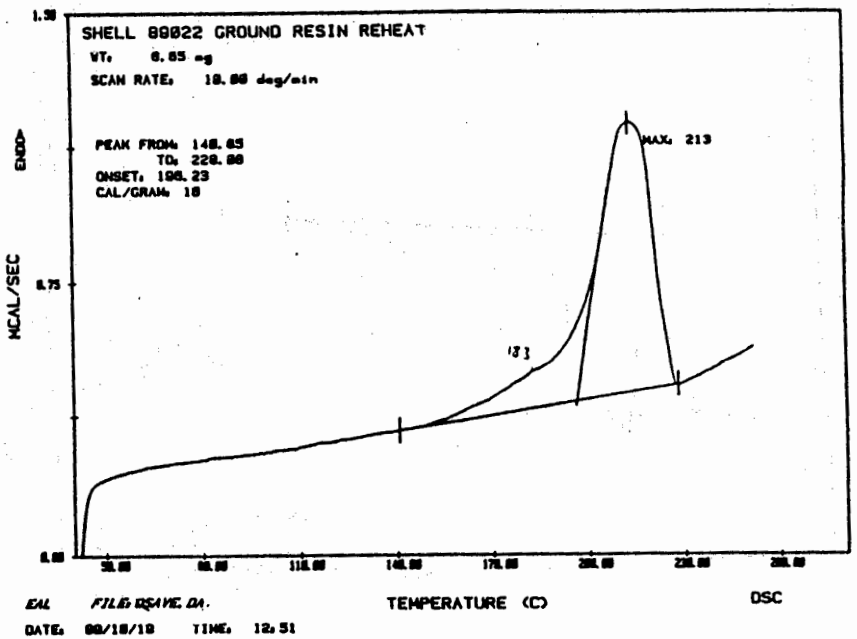

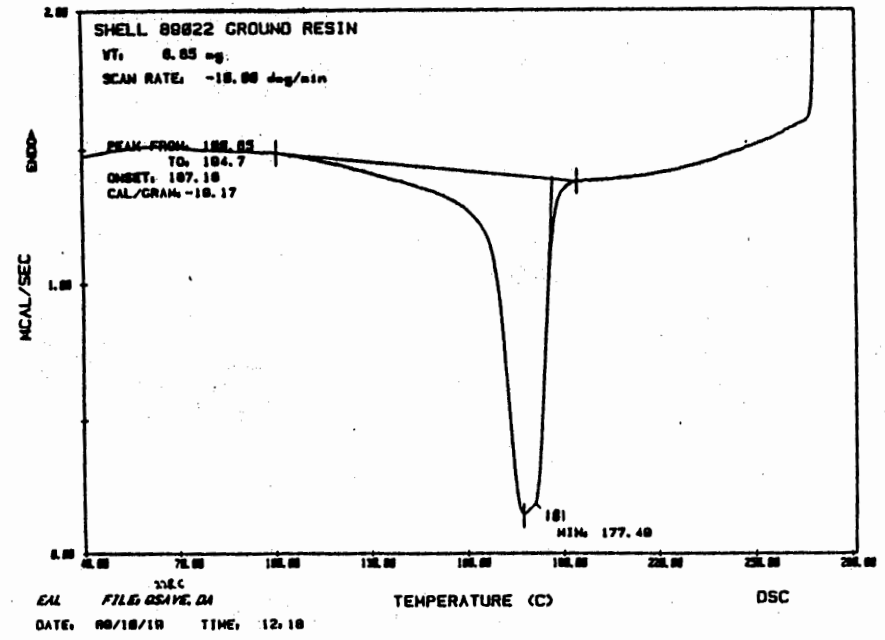

Crystallization

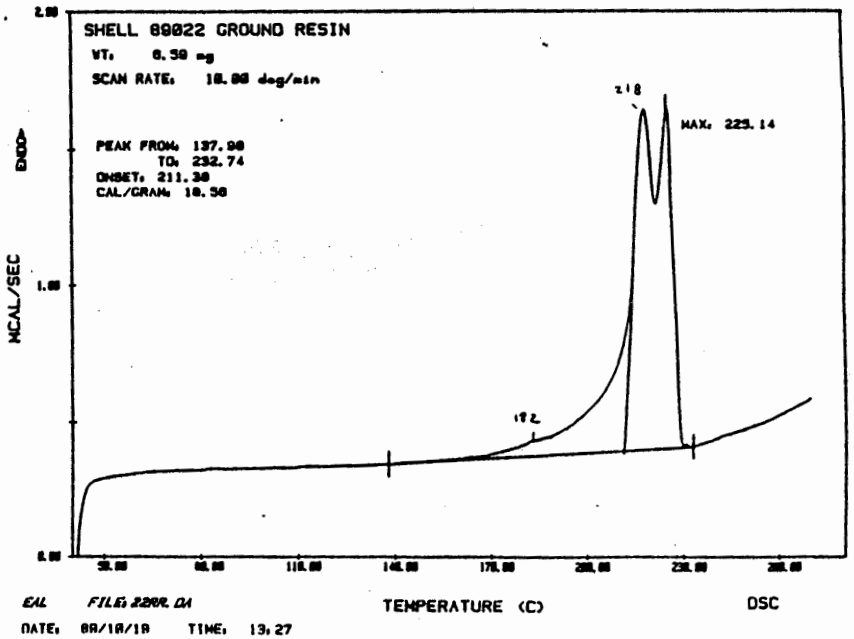

Reheat after Quench

Fig. 3

(Gr d Resin)

Initial Melting

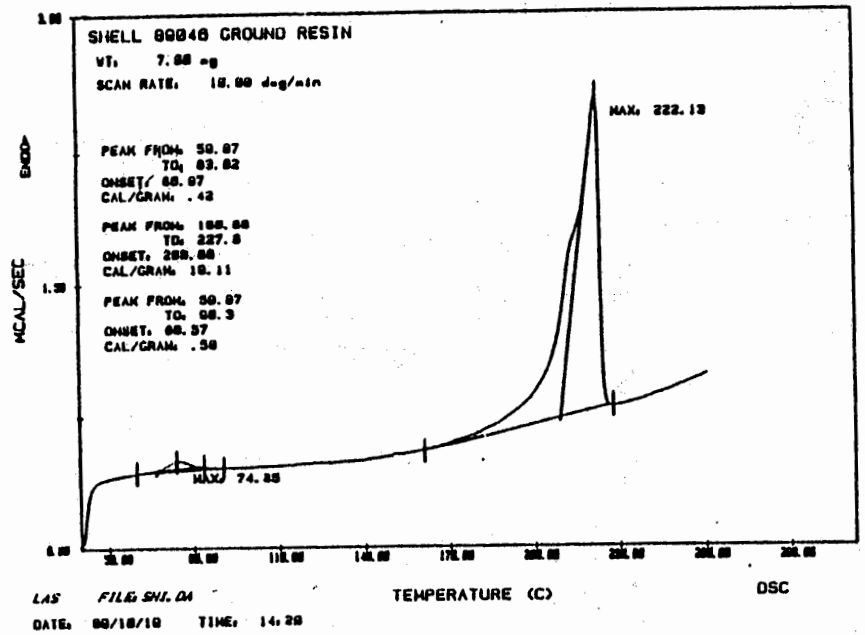

Reheat after 10°/Min. Crystallization

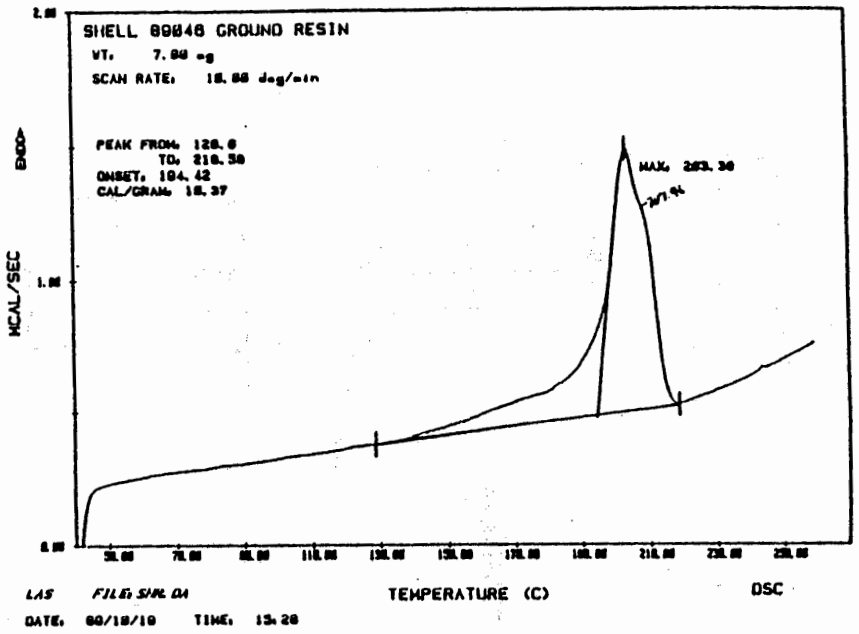

Crystallization

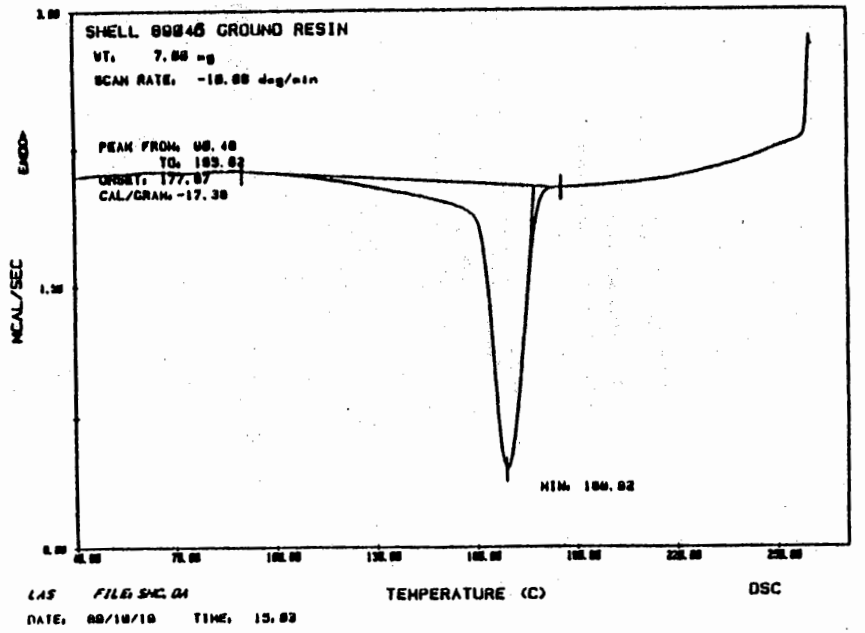

Reheat after Quench

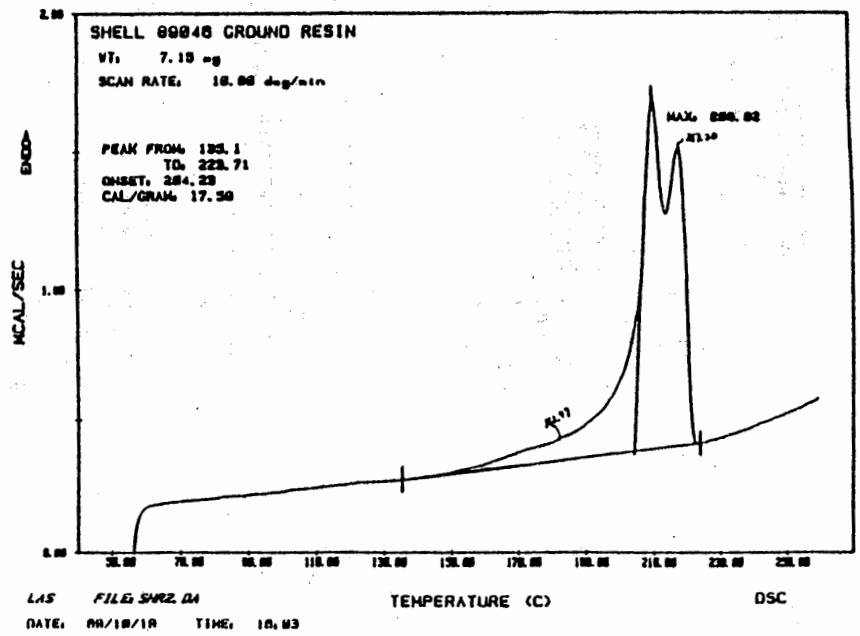

Fig. 4

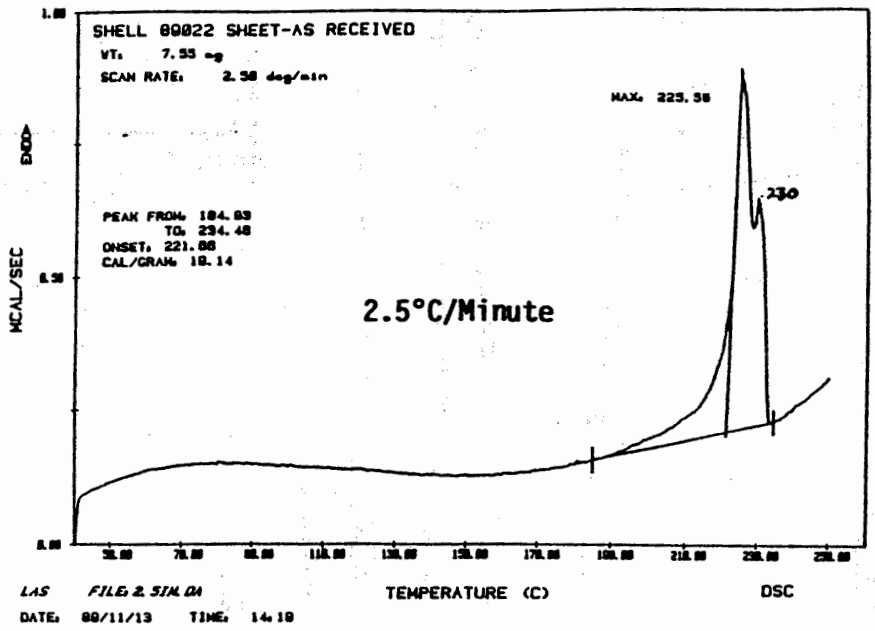

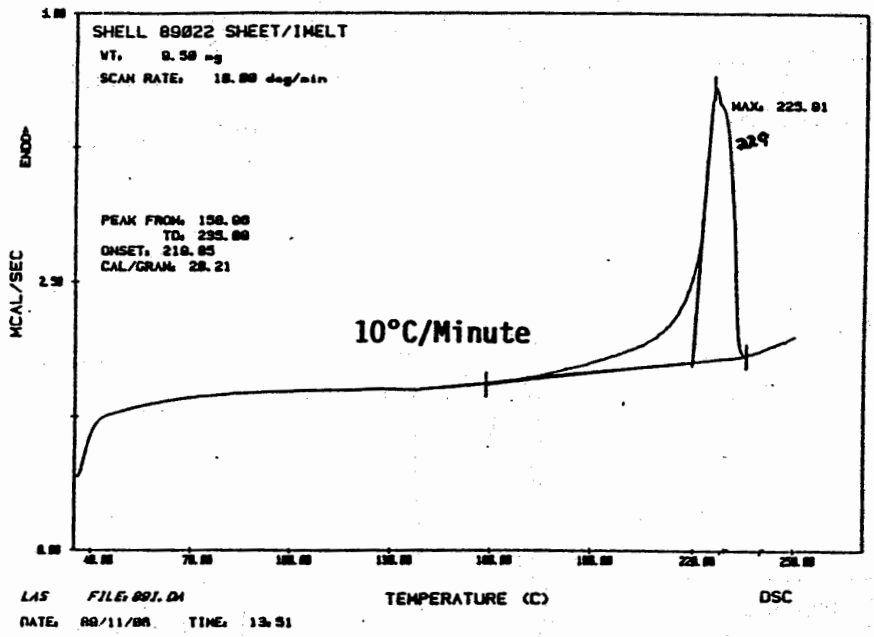

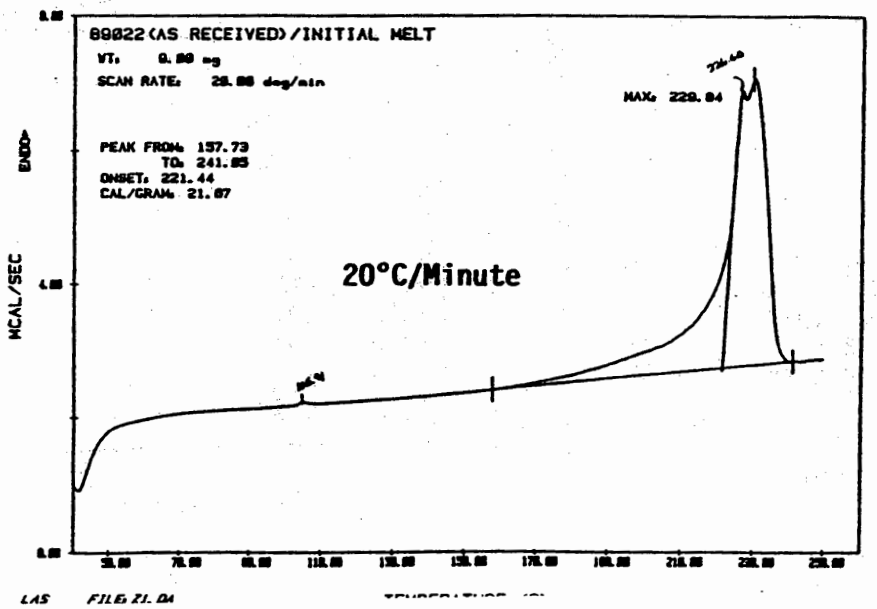

Melting as a Function of Heating Rate

Shell 89022 (Sheet - As Received

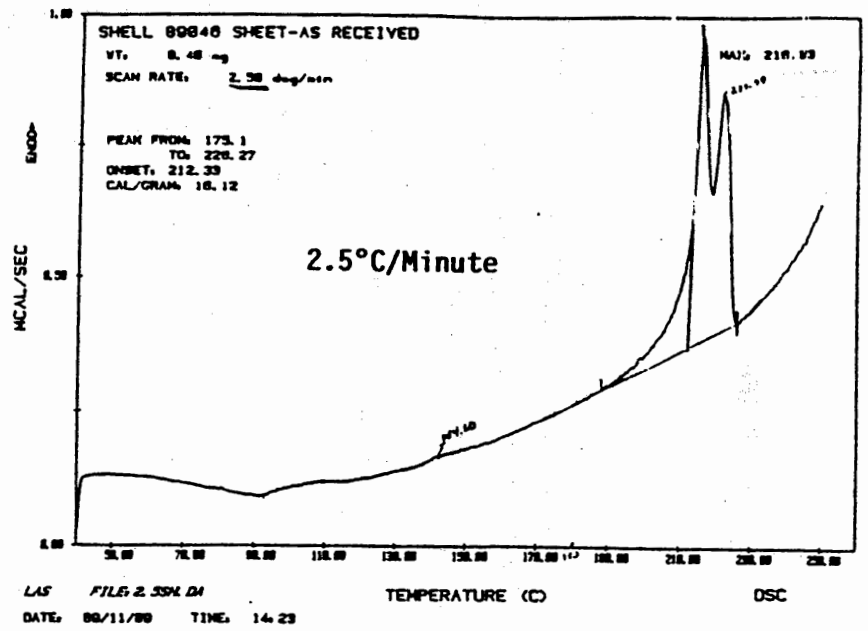

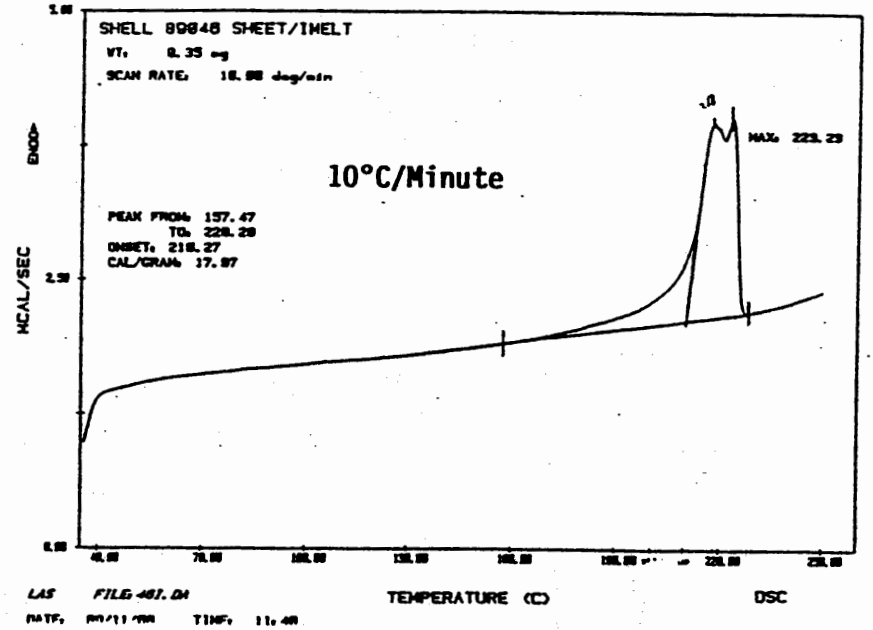

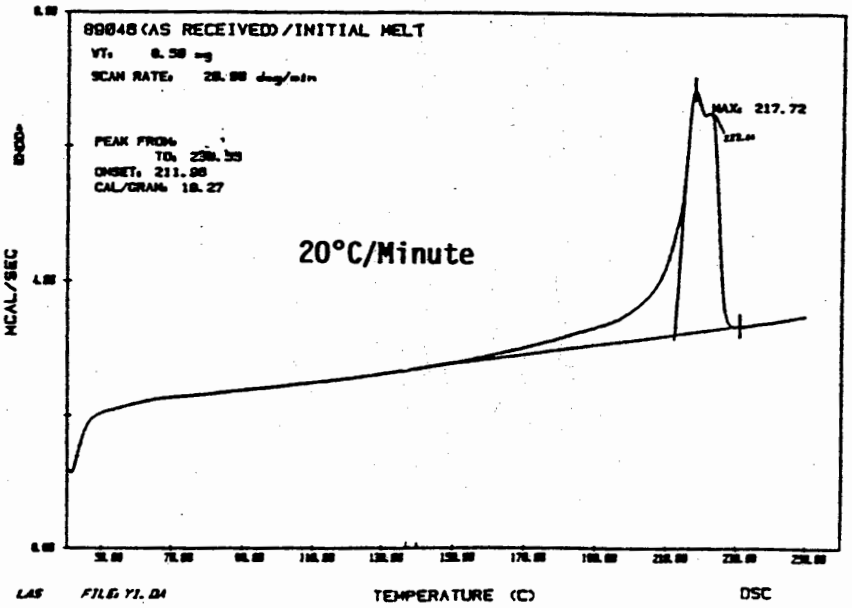

Melting as a Function of Heating Rate

Shell 89046 (Sheet - As Received)

ig. 6

Sh . 89022
(Sheet - as received)

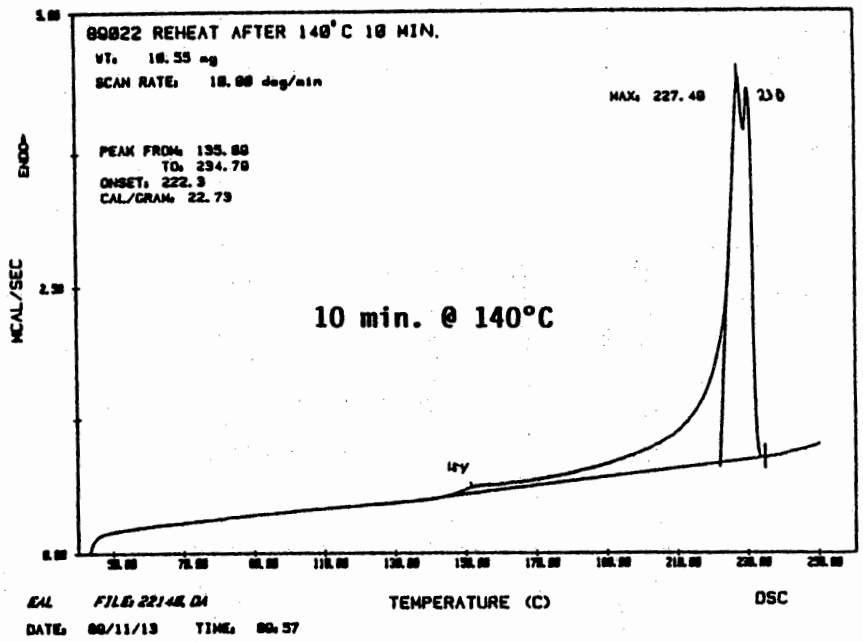

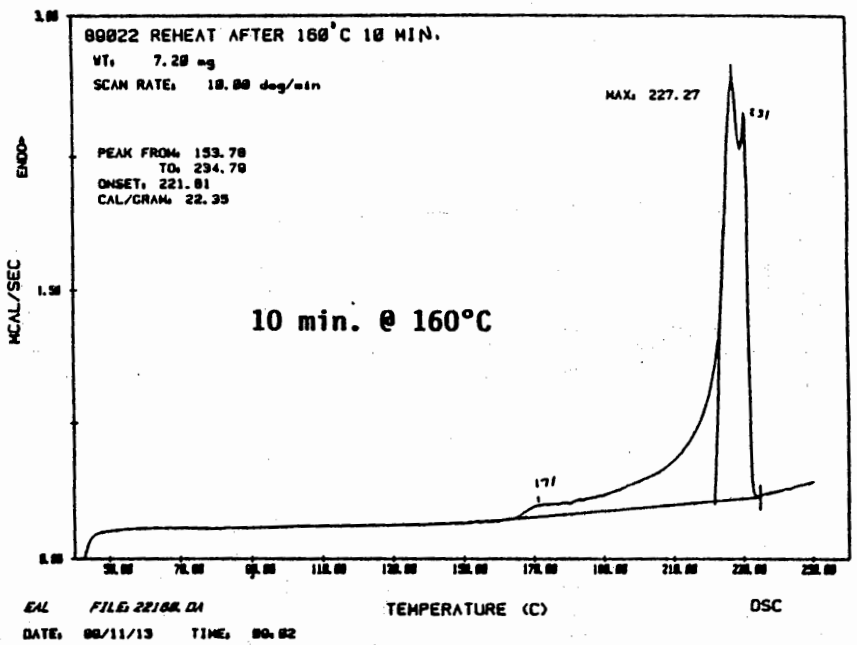

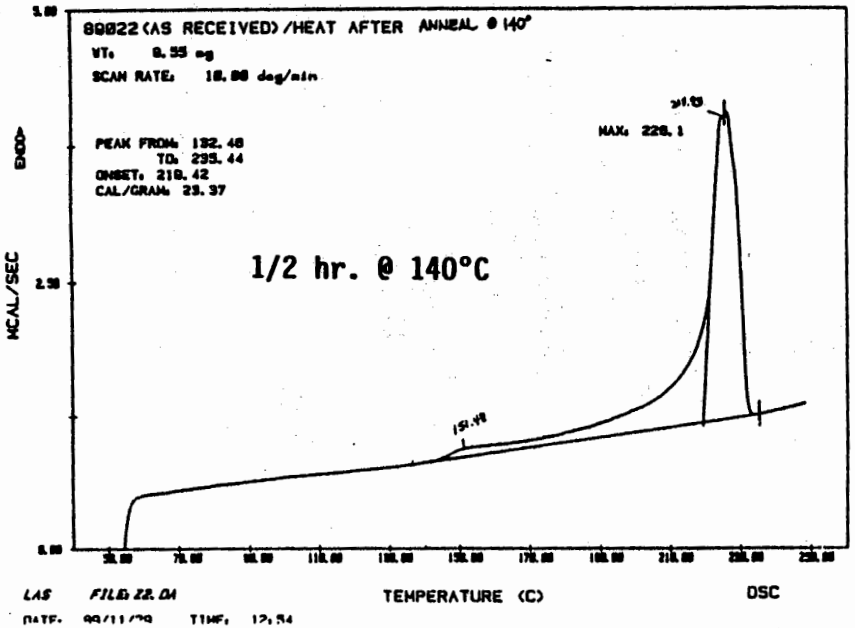

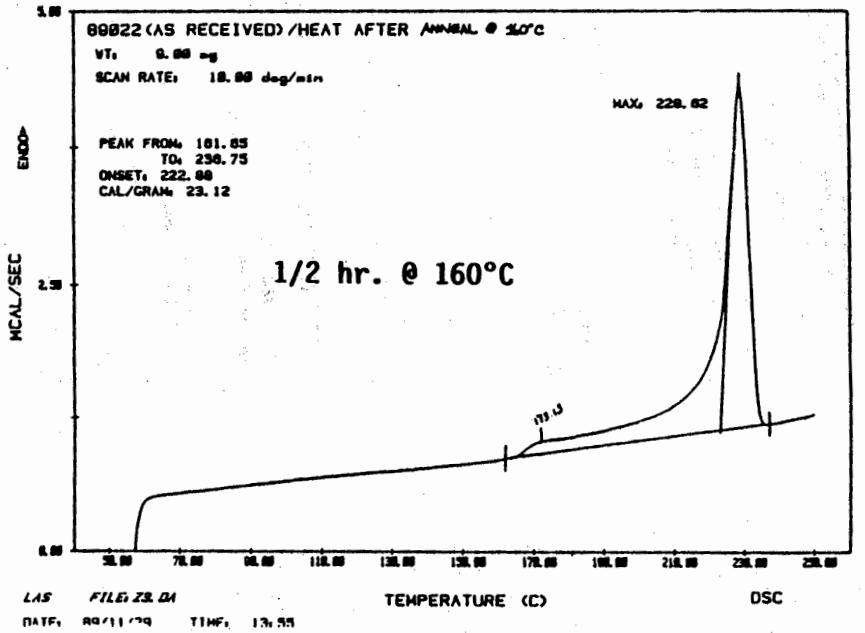

18

Fig. 7

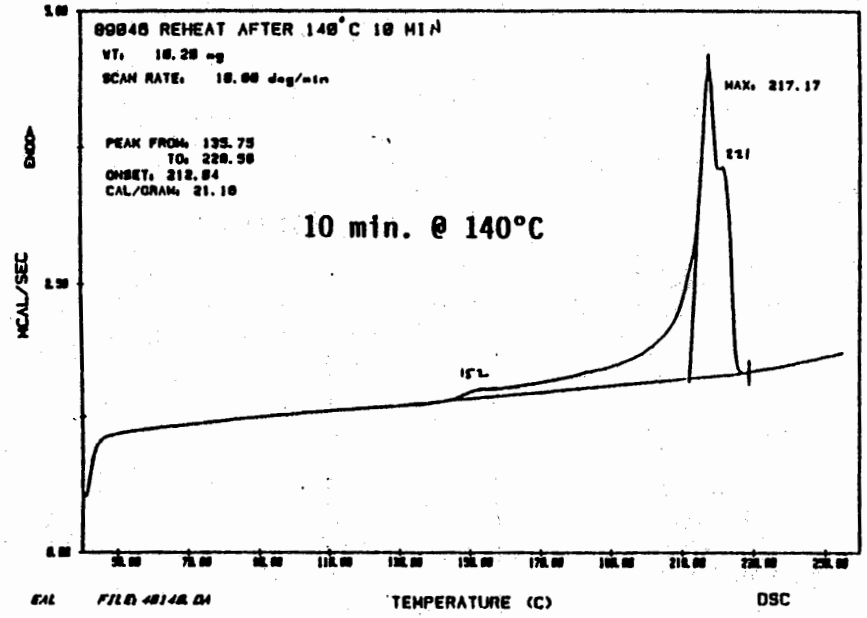
89046 REHEAT AFTER 140°C 10 MIN
WT: 10.20 mg
SCAN RATE: 10.00 deg/min
PEAK FROM: 135.75
TO: 220.50
ONSET: 212.84
CAL/GRAM: 21.10
MAX: 217.17
10 min. @ 140°C
ENDO
MCAL/SEC
TEMPERATURE (C)
DSC
DATE: 00/11/13 TIME: 10:47

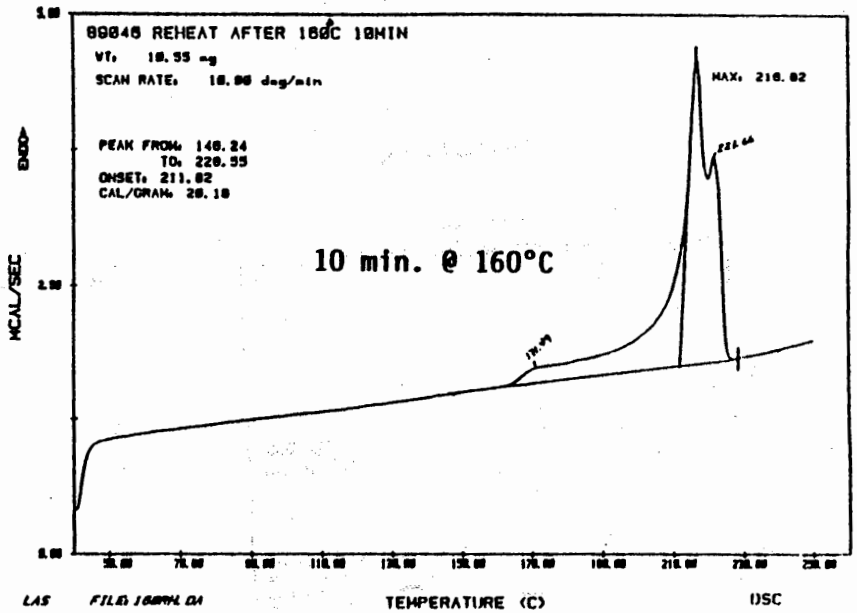
89046 REHEAT AFTER 160C 10MIN
WT: 10.55 mg
SCAN RATE: 10.00 deg/min
PEAK FROM: 140.24
TO: 220.55
ONSET: 211.02
CAL/GRAM: 20.10
MAX: 216.02
10 min. @ 160°C
ENDO
MCAL/SEC
TEMPERATURE (C)
DSC
DATE: 00/11/13 TIME: 11:43

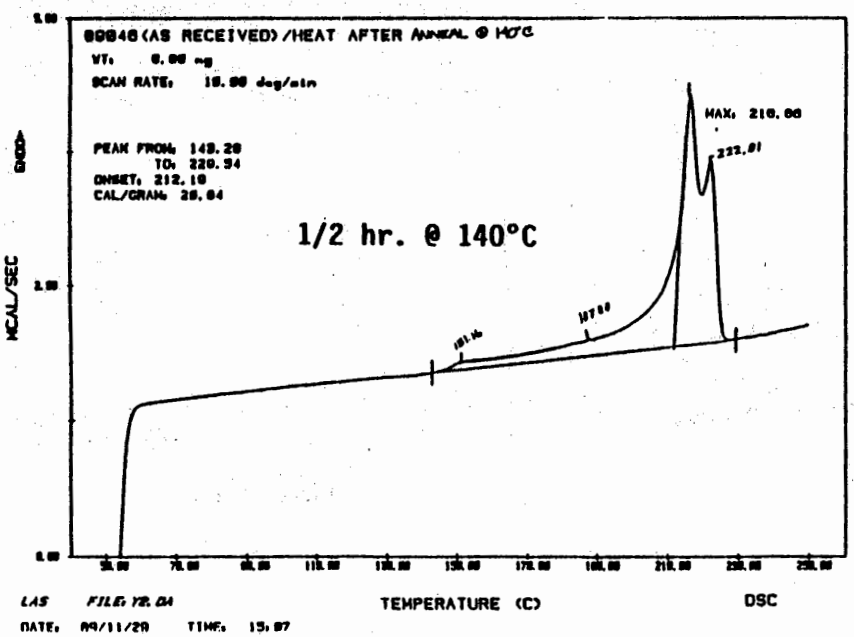
89046 (AS RECEIVED) /HEAT AFTER ANNEAL @ 140°C
WT: 9.90 mg
SCAN RATE: 10.00 deg/min
PEAK FROM: 143.20
TO: 220.94
ONSET: 212.10
CAL/GRAM: 20.04
MAX: 216.66
1/2 hr. @ 140°C
ENDO
MCAL/SEC
TEMPERATURE (C)
DSC
DATE: 00/11/20 TIME: 15:07

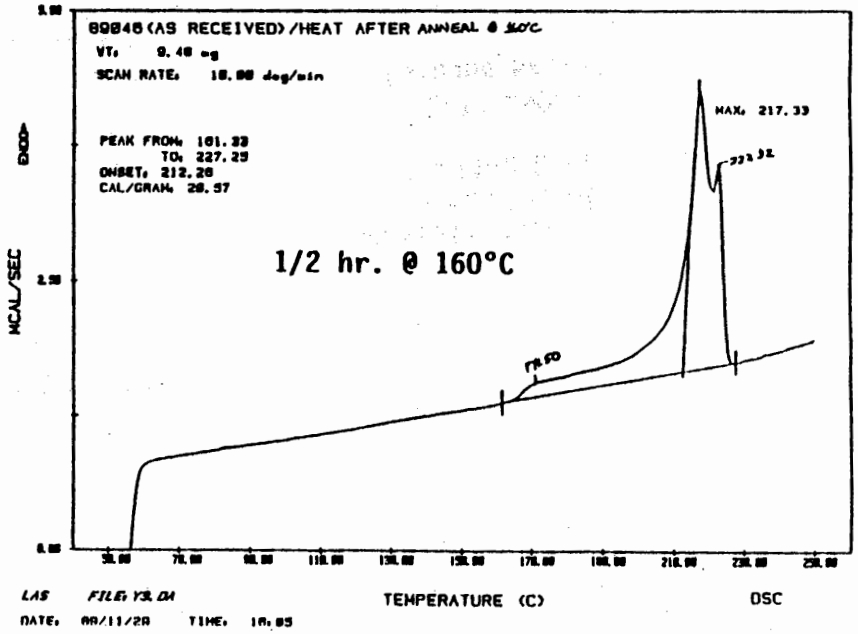
89046 (AS RECEIVED) /HEAT AFTER ANNEAL @ 160°C
WT: 9.40 mg
SCAN RATE: 10.00 deg/min
PEAK FROM: 161.33
TO: 227.29
ONSET: 212.20
CAL/GRAM: 20.57
MAX: 217.33
1/2 hr. @ 160°C
ENDO
MCAL/SEC
TEMPERATURE (C)
DSC
DATE: 00/11/20 TIME: 16:05

19

ig. 8

5°C/minute

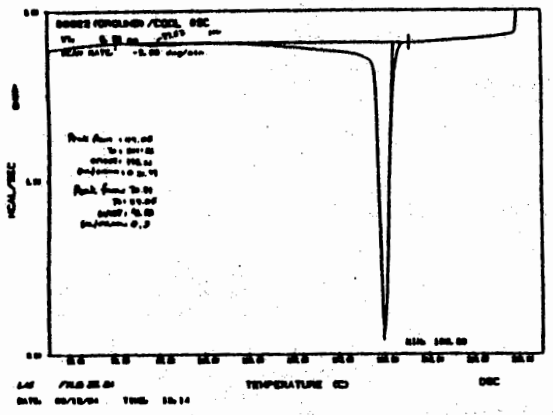

20°C/minute

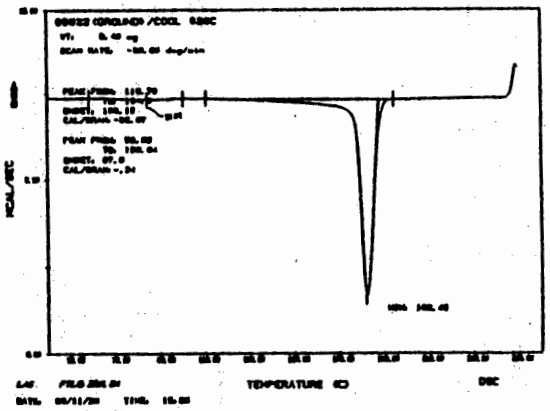

Crystallization as a function of Cooling Rate

Shell 89022 (Ground Resin)

10°C/minute

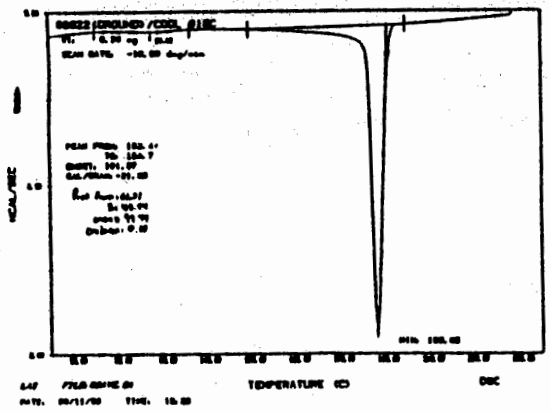

40°C/minute

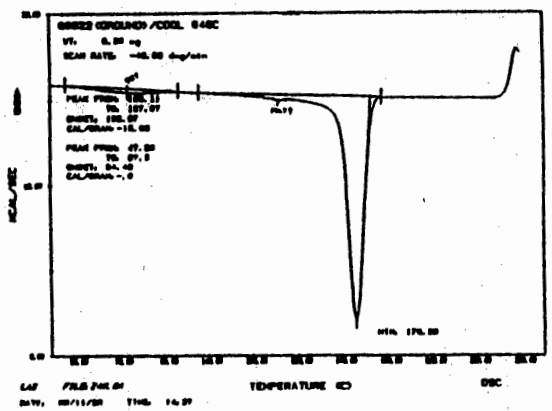

80°C/minute

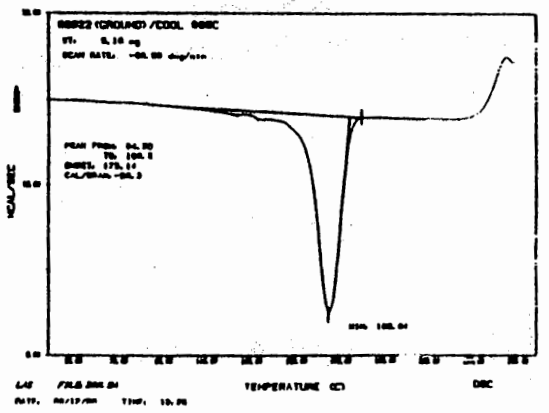

Fig. 9

5°C/minute

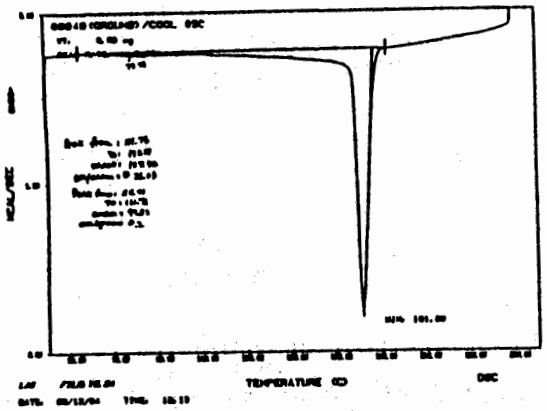

20°C/minute

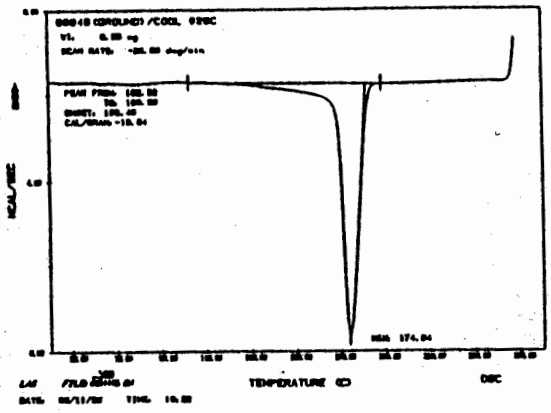

Crystallization as
a function of
Cooling Rate

Shell 89046
(Ground Resin)

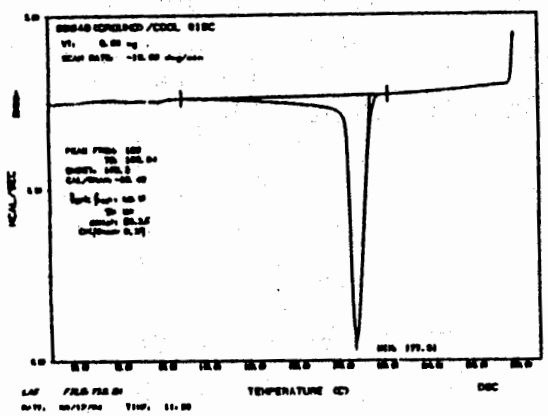

10°C/minute

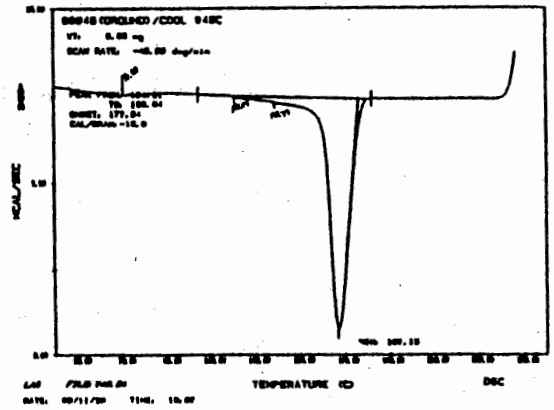

40°C/minute

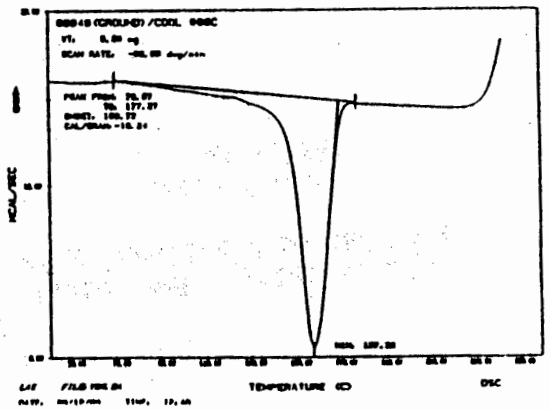

80°C/minute

Fig. 10

Isothermal Crystallization after cooling from the Melt

Shell 89022 (Ground Resin)

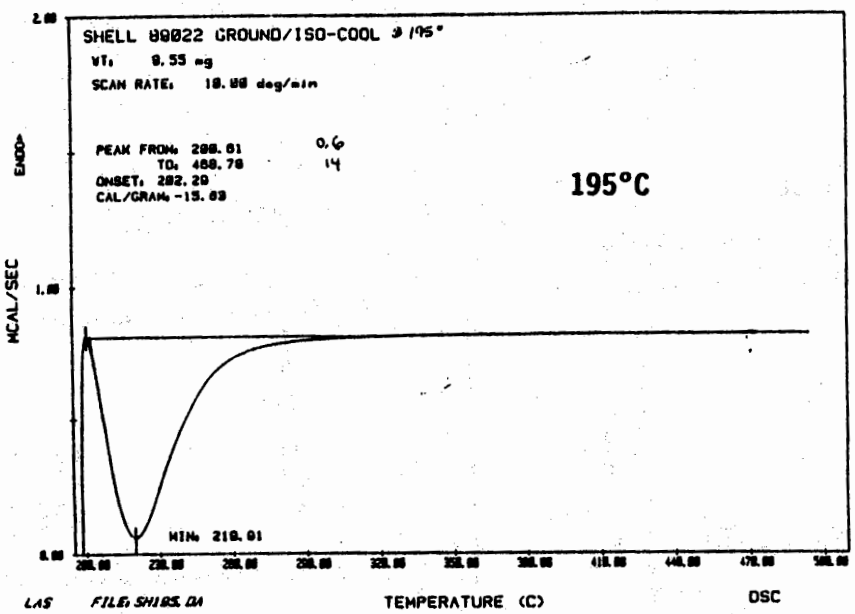

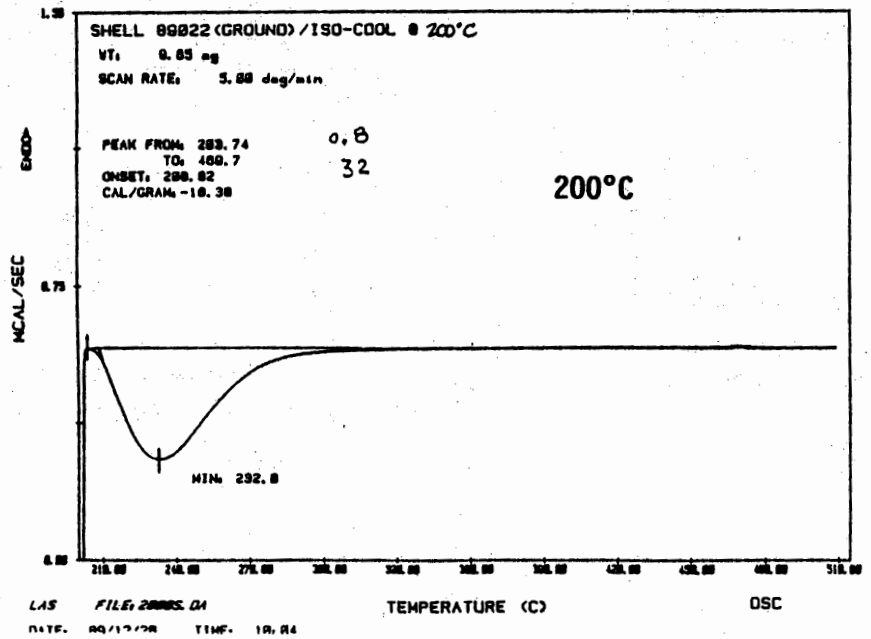

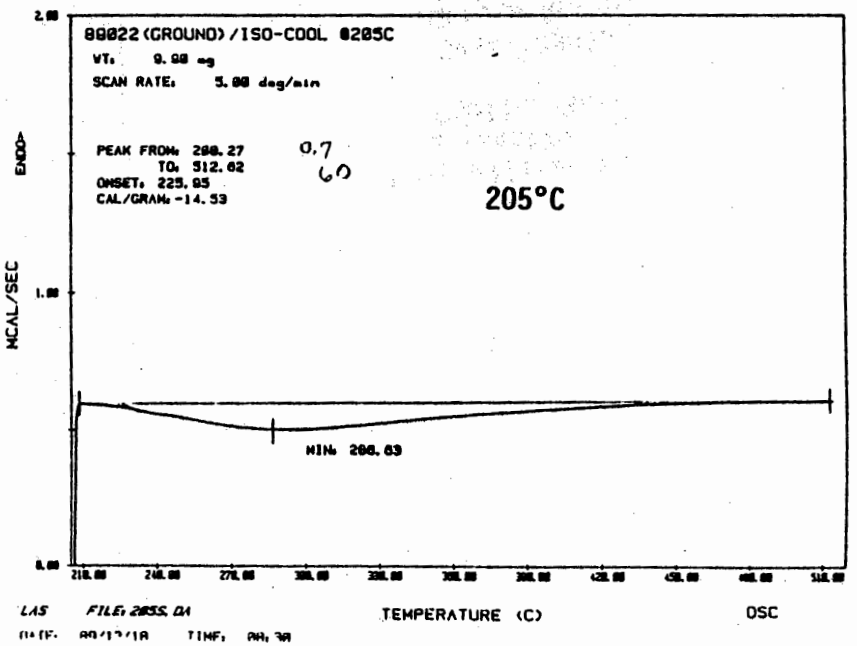

Fig. 11

after cooli _ from the Melt

Shell 89046
(Ground Resin)

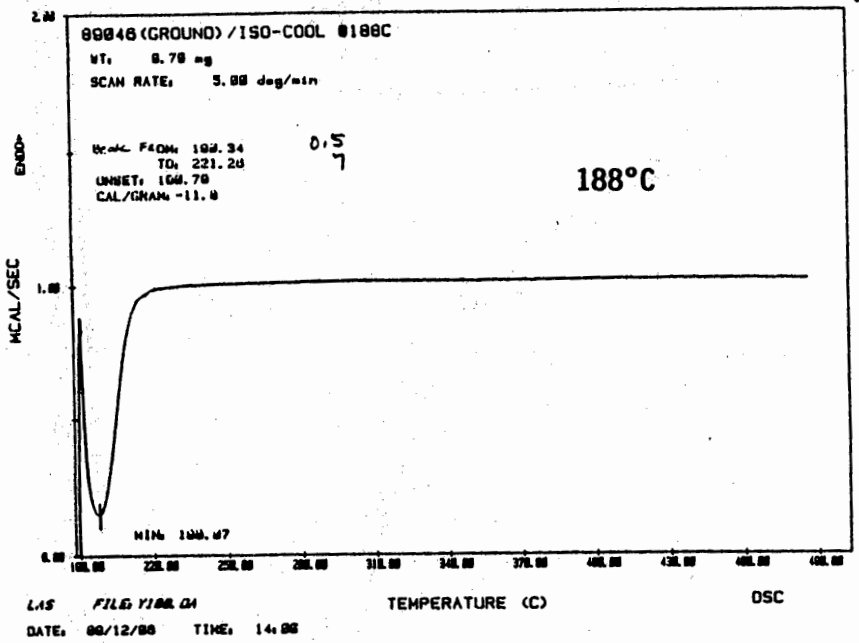

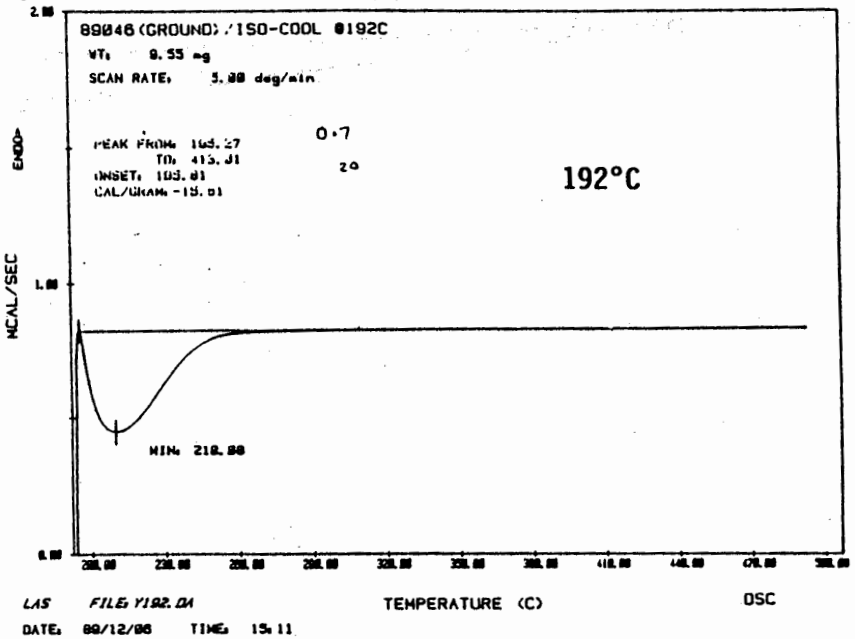

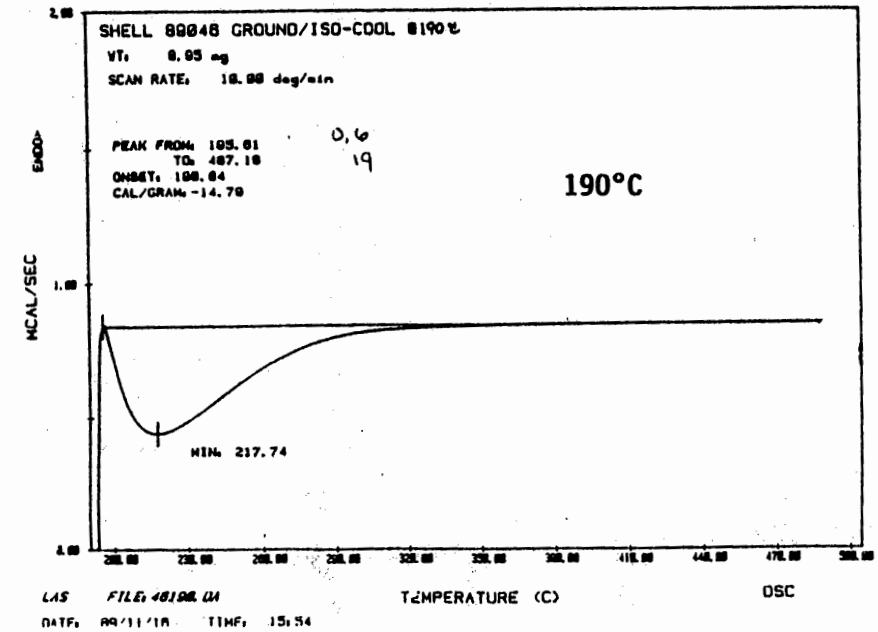

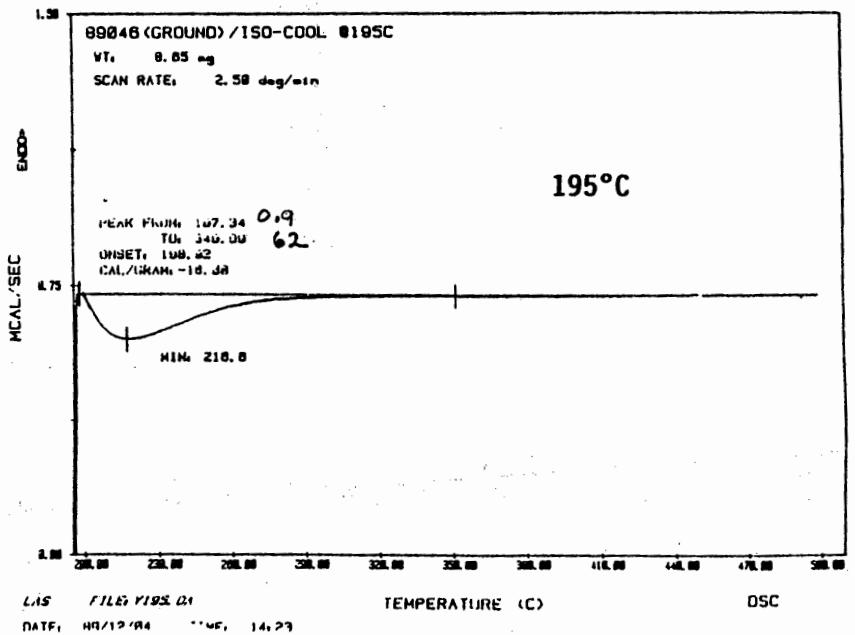

Fig. 12

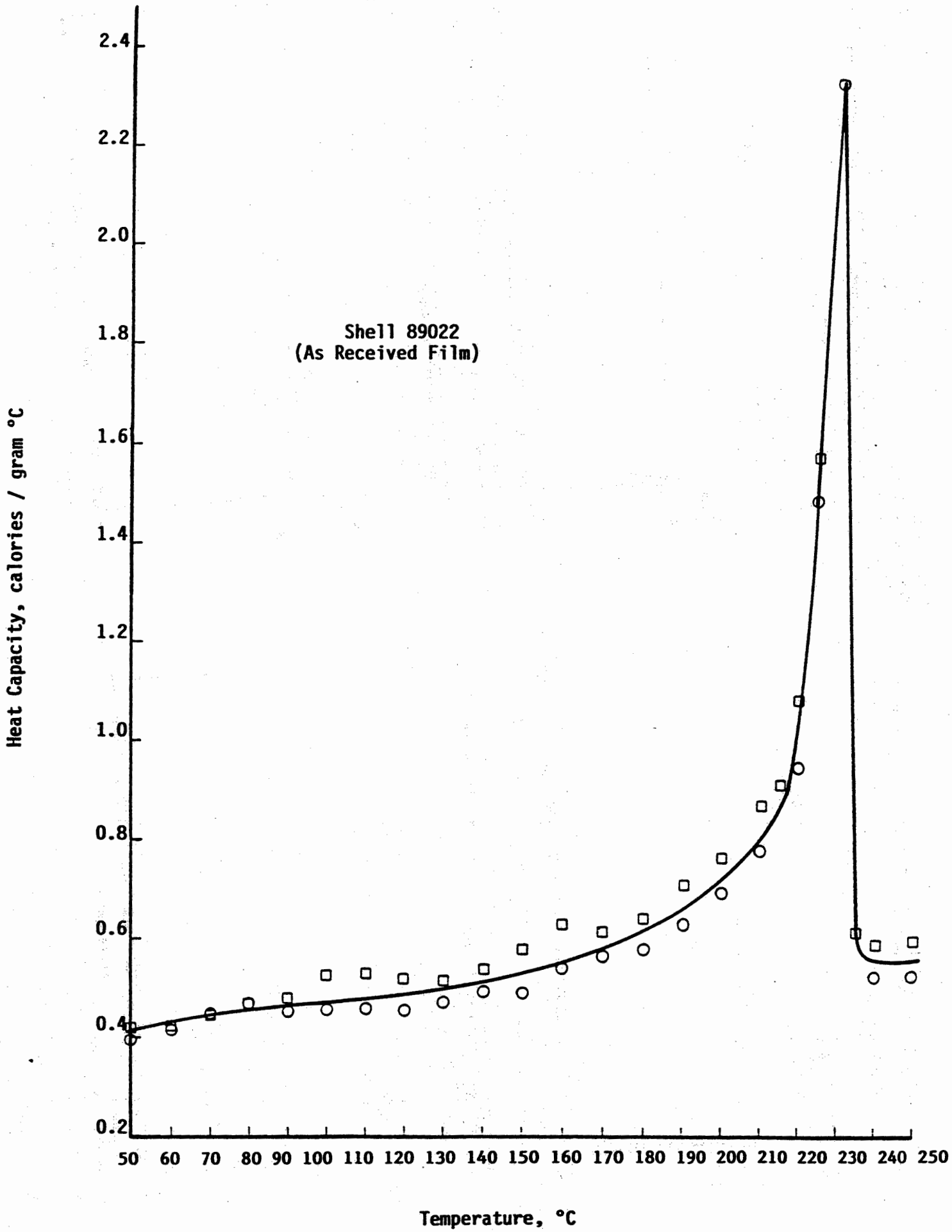
Shell 89022
(As Received Film)
Heat Capacity, calories / gram °C
2.4
2.2
2.0
1.8
1.6
1.4
1.2
1.0
0.8
0.6
0.4
0.2
50 60 70 80 90 100 110 120 130 140 150 160 170 180 190 200 210 220 230 240 250
Temperature, °C

Fig. 13

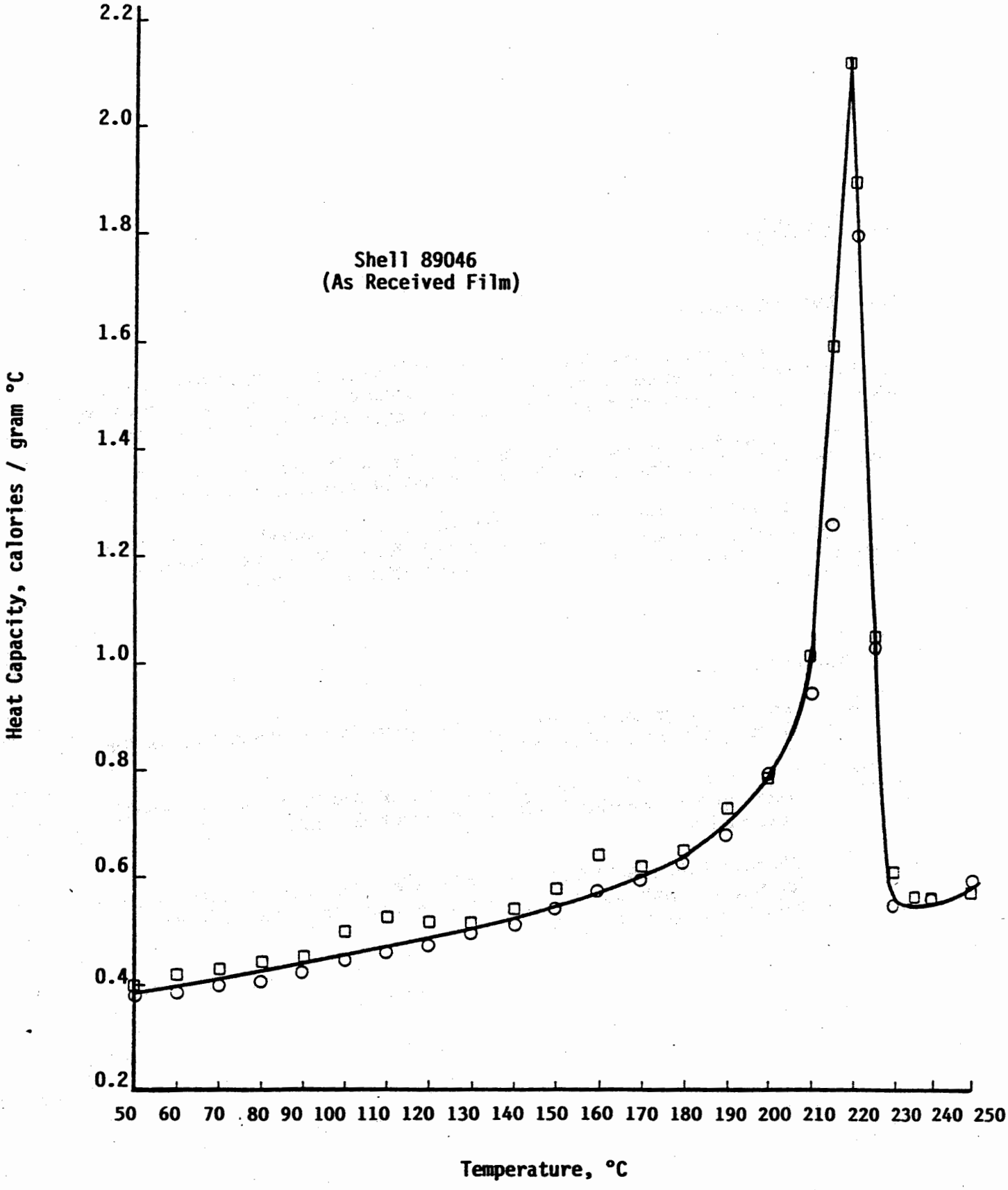
Shell 89046
(As Received Film)
Heat Capacity, calories / gram °C
2.2
2.0
1.8
1.6
1.4
1.2
1.0
0.8
0.6
0.4
0.2
50 60 70 80 90 100 110 120 130 140 150 160 170 180 190 200 210 220 230 240 250
Temperature, °C

Fig. 14

2.0 Rheology

2.1 Introduction

The Shell Proprietary Resins, Shell 89046 and Shell 89022 have been tested for the rheological properties of melt stability, steady-state viscosity and dynamic melt properties as a function of temperature and shear rate.

This information is presented in order to aid in the prediction of processing properties and to aid in the design of processing flow channels.

The viscosity of each resin is determined with respect to shear rate and temperature. Viscosity versus shear rate flow curves are offered as an aid for flow channel design and as a prediction for processing properties.

2.2 Conclusions

- Thermal Degradation, while in the melt, is the controlling factor in melt rheology measurements.
- Processing of Shell Proprietary resins should be at the lowest temperature possible (≈240°C) in order to minimize melt degradation.
- The Shell Resins, 89022 and 89044 are both characterized as having low melt strength. For free extrusion blow molding, this could be a problem.

2.3 Results and Discussion

2.31 Melt Stability

A. Introduction

Melt Stability is a measure of changes to the polymer that occur at melt temperatures. Viscosity is an indicator of those changes to the molecular structure of the polymer. Molecular enlargement or chain scission are two of the most common changes that can occur.

In order to determine the suitability for processing a resin, the melt stability of each resin is calculated. It is very important during melt processing, that the polymer not degrade. Melt Stability is calculated from viscosity versus time data and is a function of the change of viscosity with respect to time. A thermally stable resin will have little change in viscosity over time.

B. Experimental

Viscosity as a function of time was recorded on the Rheometrics Visco-Elastic Tester oscillating viscometer at low shear rate and at the expected processing temperature. Conditions of the test were:

Rheometrics Visco-Elastic Tester (RVE)
25mm parallel plates
strain: 15%
frequency: .1 rad/s
temp: 240°C, 250°C, 260°C
Atmosphere: nitrogen

Viscosity and Time data at each temperature is fitted to a linear least square equation. The following equation is used:

$$\ln(\eta) = A + B \times Time$$

η = viscosity (poise)
A = intercept ($\ln \eta$)
B = slope($\ln \eta$ / time)
time = minutes

In this determination of melt stability, the important number is the slope of the curve. Large values of slope signify large amounts of thermal degradation.

C. Results

The results of melt stability measurements are presented in Table VII, and Figure 15, Figure 16. As shown by the data, the Shell resins, 89022 and 89044 are very degradable at processing temperatures. For best processing and melt stability, the melt temperature should be 240°C.

Table VII Melt Stability of Shell Resins

Shell Resin	Temperature (°C)	Linear Slope ($\ln\eta$/min)
89022	240	0.0609
	250	0.0911
	260	0.1152
89046	240	0.0597
	250	0.0835
	260	0.0896

Figure 15 **Melt Stability of Shell 89022**

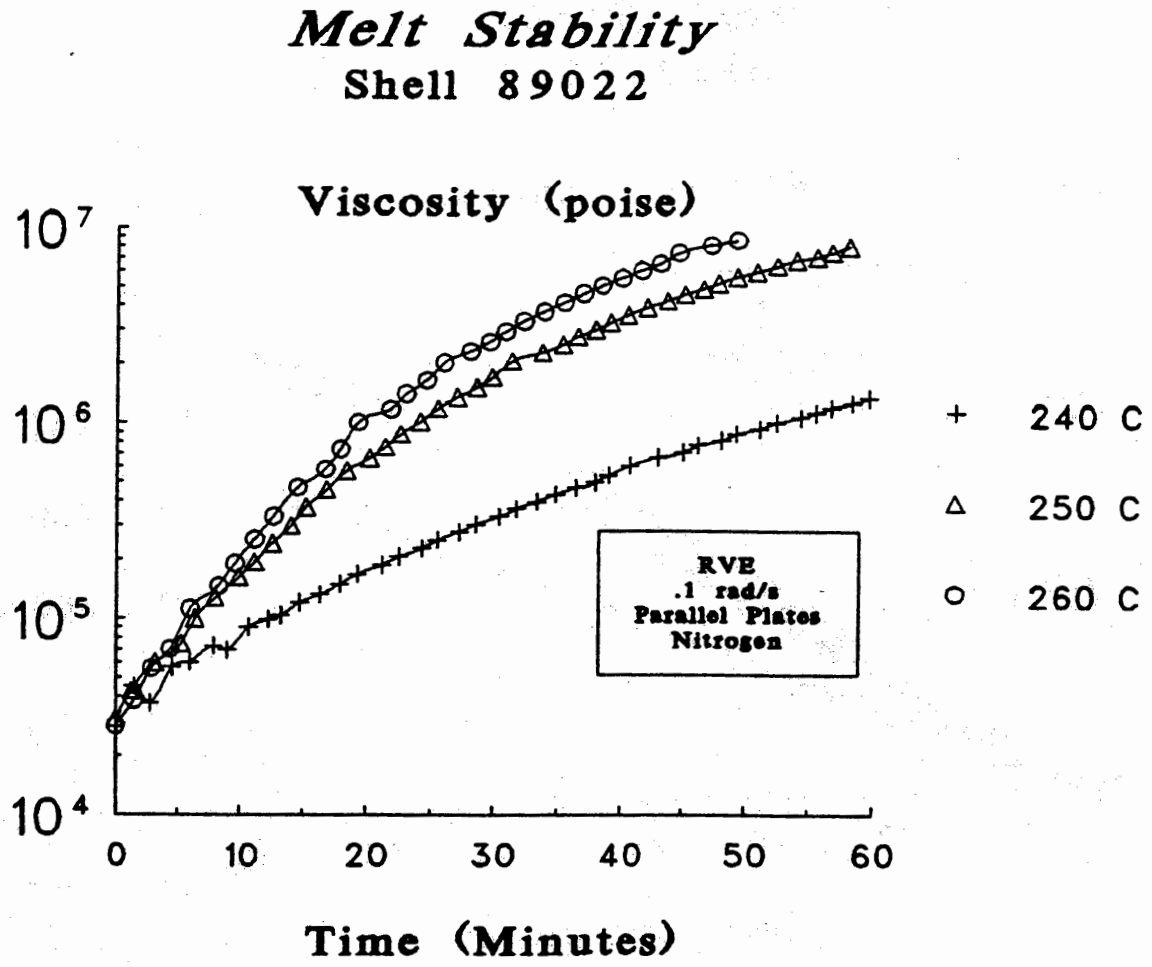

Figure 16 **Melt Stability of Shell 89046**

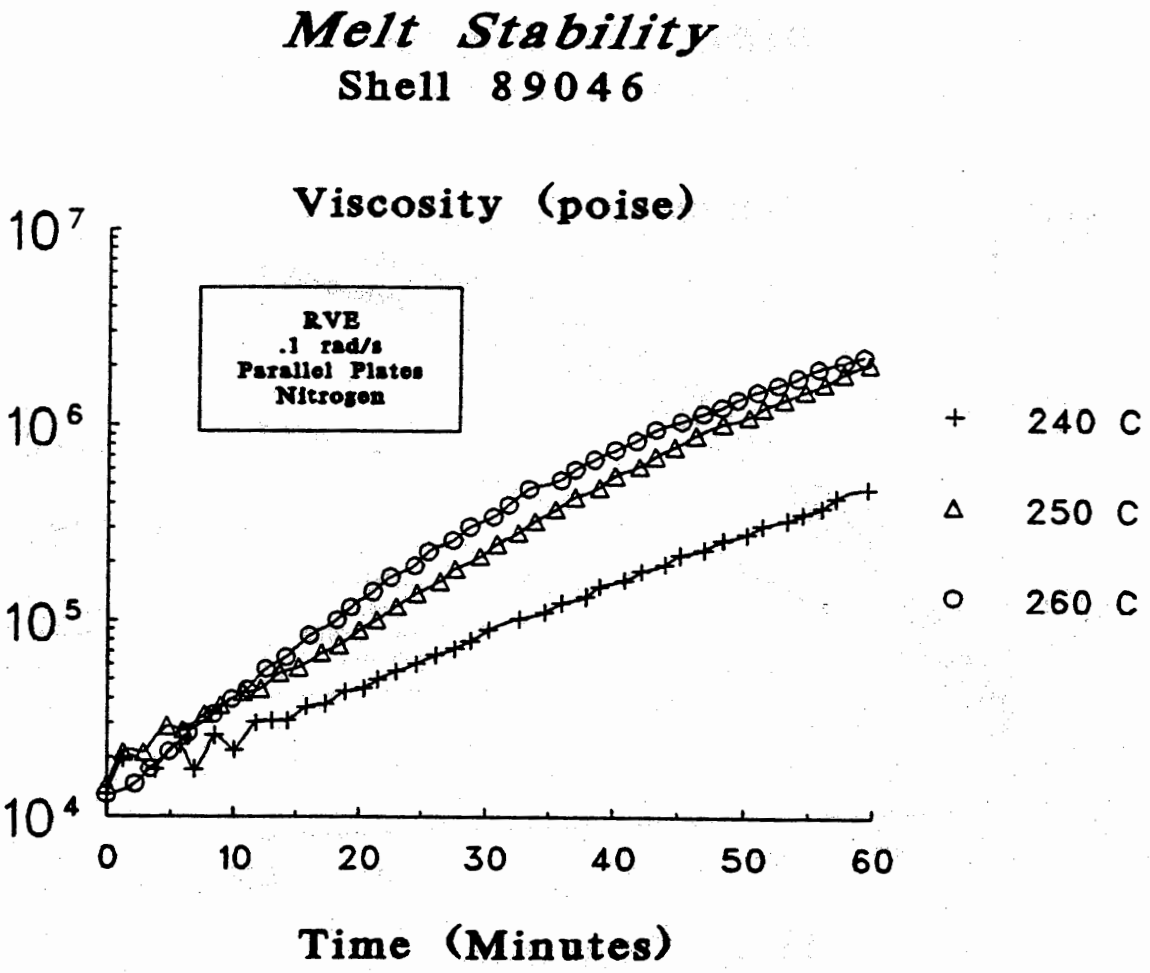

2.32 Steady-State Viscosity

A. Introduction

Steady State Viscosity as a function of shear rate and temperature was determined in order to build mathematical models of polymer flow and as an aid for prediction of processing properties.

The two Shell Resins, 89022 and 89046, were tested for viscosity by a capillary rheometer at three temperatures.

B. Experimental

Instron Capillary Rheometer
Die: .0402 x .8248 inch
Temperature: 240°C, 250°C, 260°C

C. Results and Discussion

The Results are presented in Table VIII and, Figure 17 and Figure 18.

Thermal degradation was a major factor in the measurement of viscosity. The viscosity for both materials at 260°C, was greater than the viscosity at 240°C, despite the temperature thinning effect. This can be attributed to thermal degradation being greater at 260°C than at 240°C.

Thermal degradation of the polymers is also greater when measuring at low shear rates because of the longer time needed to make the measurement.

Table VIII Steady State Viscosity of Shell Resins

Shell Resin	Temp (°C)	η 1 sec^{-1} (Kpoise)	η 1000 sec^{-1} (Kpoise)	Shear Sensitivity (1/1000)	Curve Fitting Constants
89022	240	162.5	2.93	55.4	A= 5.2110 B=-0.7622 C= 0.0603
	250	105.7	2.32	45.6	A= 5.0240 B=-0.7245 C= 0.0572
	260	177.6	2.75	64.5	A= 5.2494 B=-0.7410 C= 0.0459
89046	240	76.9	2.29	33.5	A= 4.8860 B=-0.6209 C= 0.0375
	250	90.2	2.08	43.3	A= 4.9551 B=-0.7351 C= 0.0639
	260	77.3	2.10	36.8	A= 4.8883 B=-0.6191 C= 0.0324

HDPE 120 - 150 3-8

Figure 17 **Steady State Viscosity of Shell 89022**

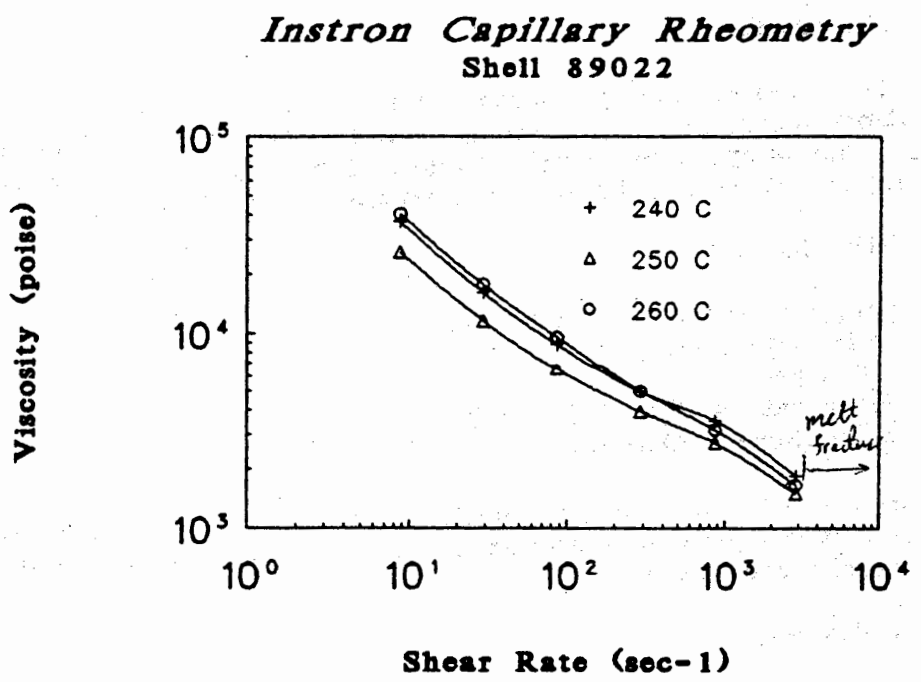

HDPE blow molding grades melt fracture above 10^3 sec^{-1} shear Rates.

Figure 18 **Steady State Viscosity of Shell 89044**

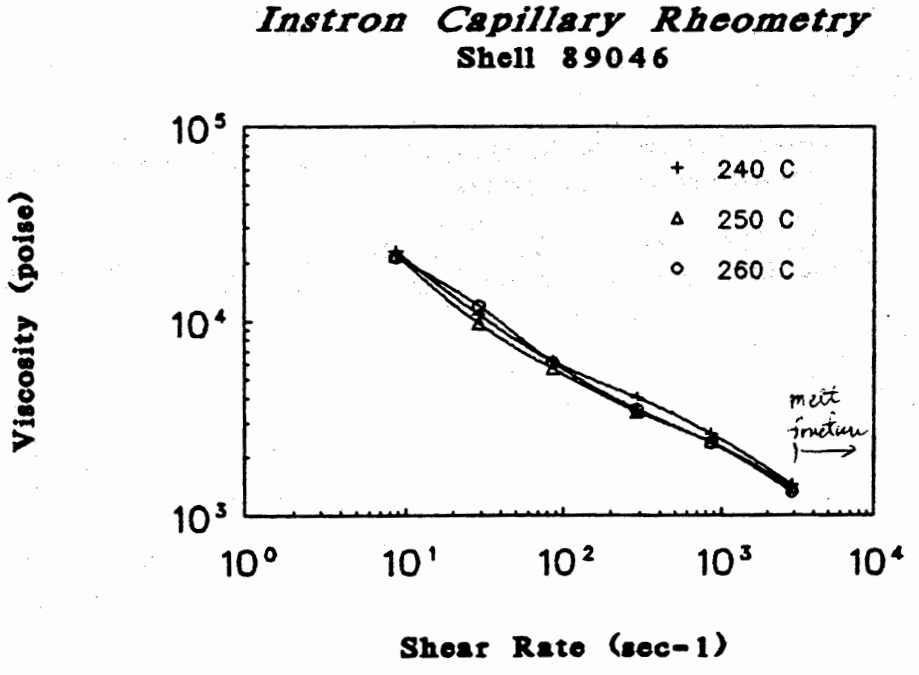

2.33 Dynamic Rheometry

A. Introduction

The dynamic melt properties, melt properties measured under oscillating shear, have been tested using a Rheometrics Visco-Elastic Tester (RVE). The purpose is to gain insight into viscosity, elasticity, and damping action as it relates to temperature and shear rate.

B. Experimental

Rheometrics Visco-Elastic Tester
25mm. cone and plate
15% strain
shear rate = .1 to 100 rad/s
atmosphere = nitrogen

G′ and G″, the storage modulus and loss modulus respectively were measured as a function of frequency (ω). From these quantities, the following are calculated:

Complex Viscosity

$$\eta^* = \sqrt{\left(\frac{G'}{\omega}\right)^2 + \left(\frac{G''}{\omega}\right)^2}$$

η^* = complex viscosity
G′ = storage modulus
G″ = loss modulus
ω = frequency (rad/s)

Tangent Delta, damping factor

$$\tan \delta = \frac{G''}{G'}$$

tan δ = tangent of the phase angle

C. Conclusions

- Thermal Stability in the melt is the major factor that influences rheological measurements.
- The Shell resins, 89022 and 89046, are both characterized as low in shear sensitivity and melt strength.

D. Results and Discussion

As stated before, thermal degradation in the melt of shell resins was a major factor in rheological determinations. For this reason, some erratic results are reported for dynamic melt properties. For example, the complex viscosity of Shell 89046 (shown in Figure 20) is less at 240°C than at 250°C. Similarly, storage modulus lines are seen to cross at a given frequency. Still, some melt characteristics can be seen.

The complex viscosity, η^*, is shown in Figure 19 and Figure 20 as a function of shear rate at different temperatures. Both Shell resins, 89022 and 89046 lack high melt strength (low shear viscosity), a desirable quantity for free extrusion blow molding. Most blow molding grades of resin have viscosity values of 1×10^5 poise or greater at 0.1 rad/s shear rate. Both shell resins have viscosity values less than 1×10^5 poise.

The storage modulus, G′, of both Shell resins is shown in Figure 21 and Figure 22. These curves are not typical because the storage modulus is seen to cross each other at different temperatures.

Tangent Delta (tan δ) versus frequency is shown in Figure 23 and Figure 24. A relaxation transition is detected for Shell 89046 and perhaps Shell 89022 between 0.1 and 1.0 rad/s at 240°C. This signifies that the materials are very close to the melting point under shear.

Figure 19 **Complex Viscosity of Shell 89022**

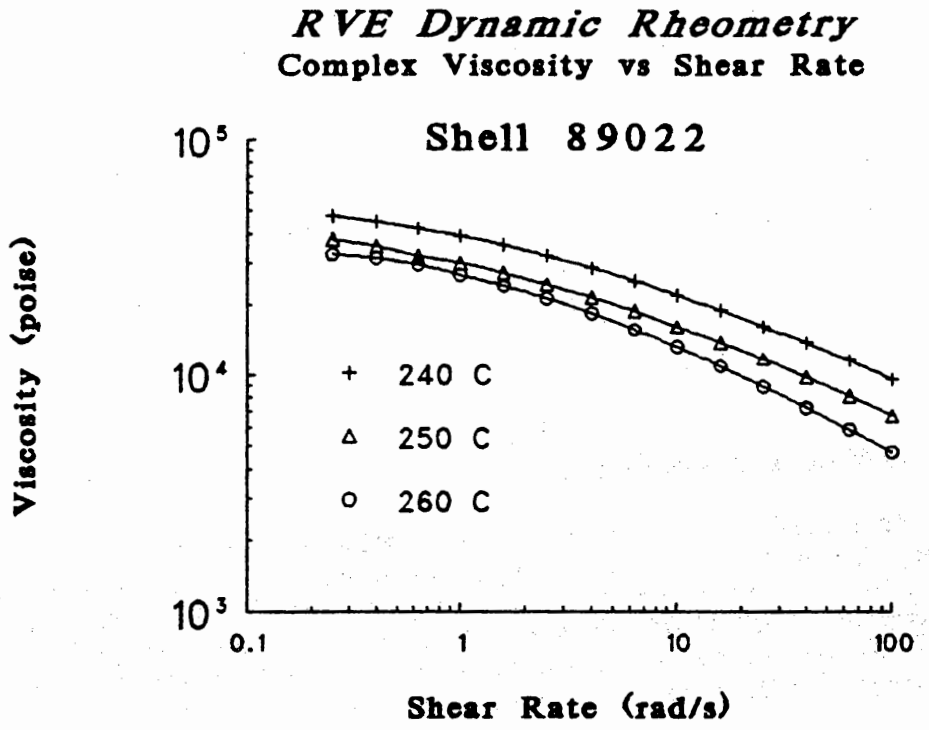

Figure 20 **Complex Viscosity of Shell 89046**

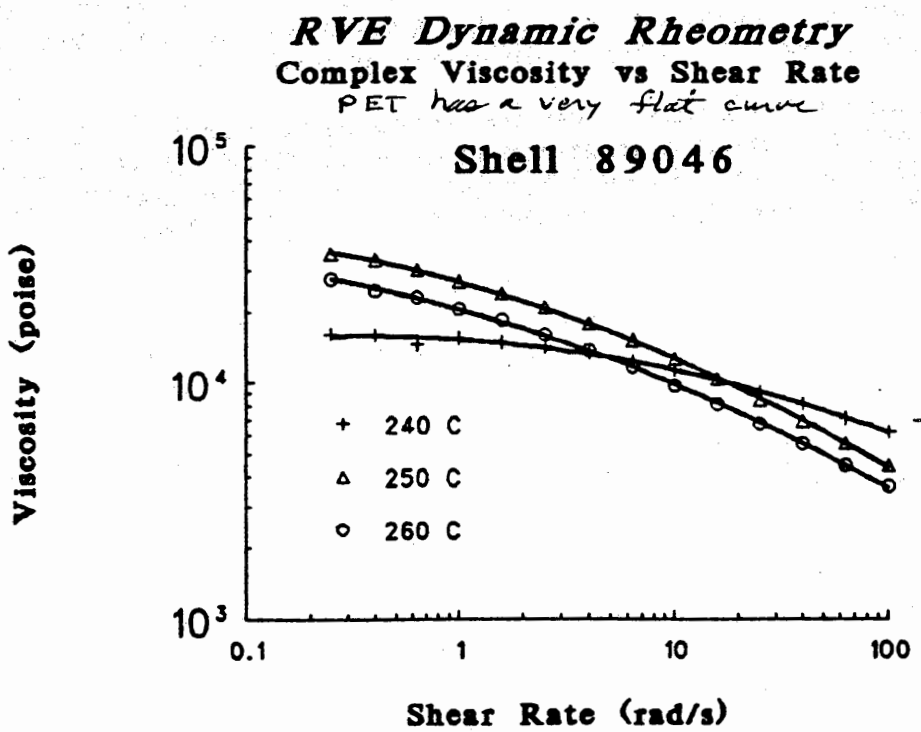

Figure 21 Storage Modulus of Shell 89022

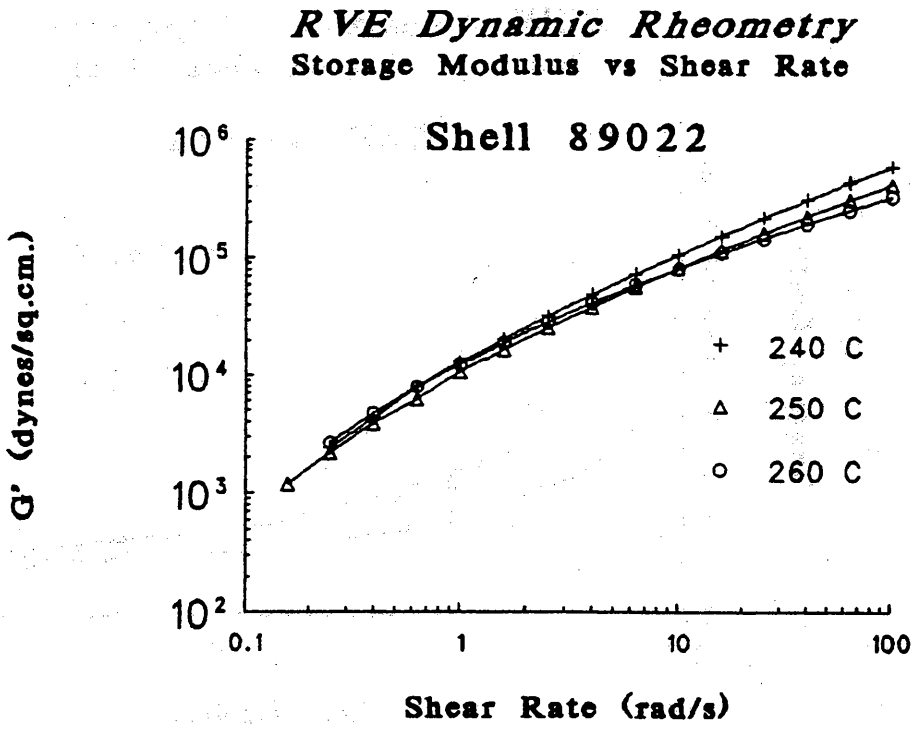

Figure 22 Storage Modulus of Shell 89046

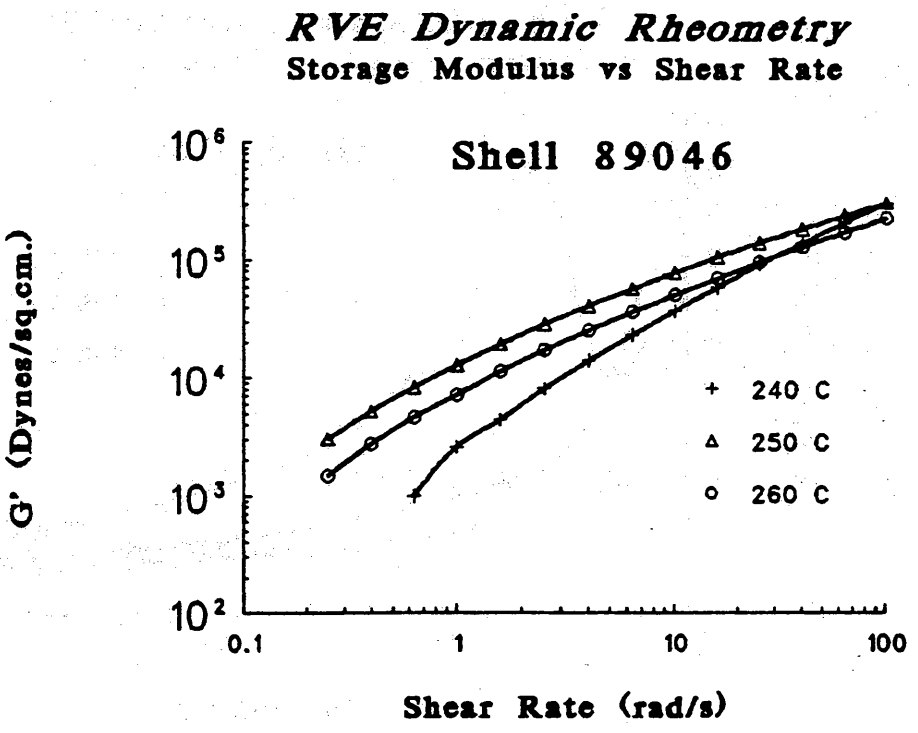

Figure 23 Tangent Delta of Shell 89022

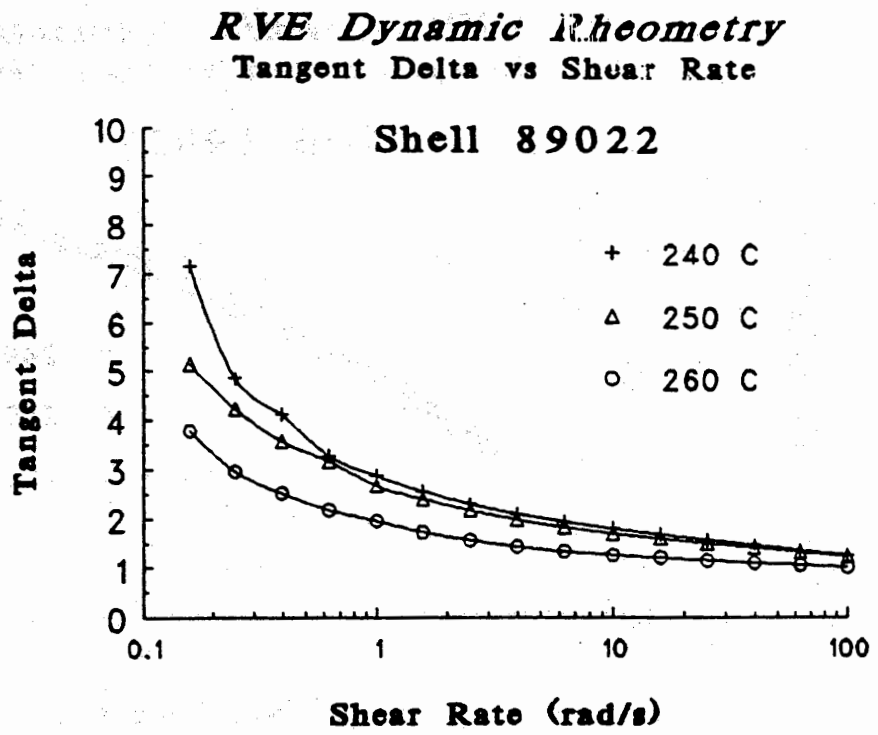

Figure 24 Tangent Delta of Shell 89046

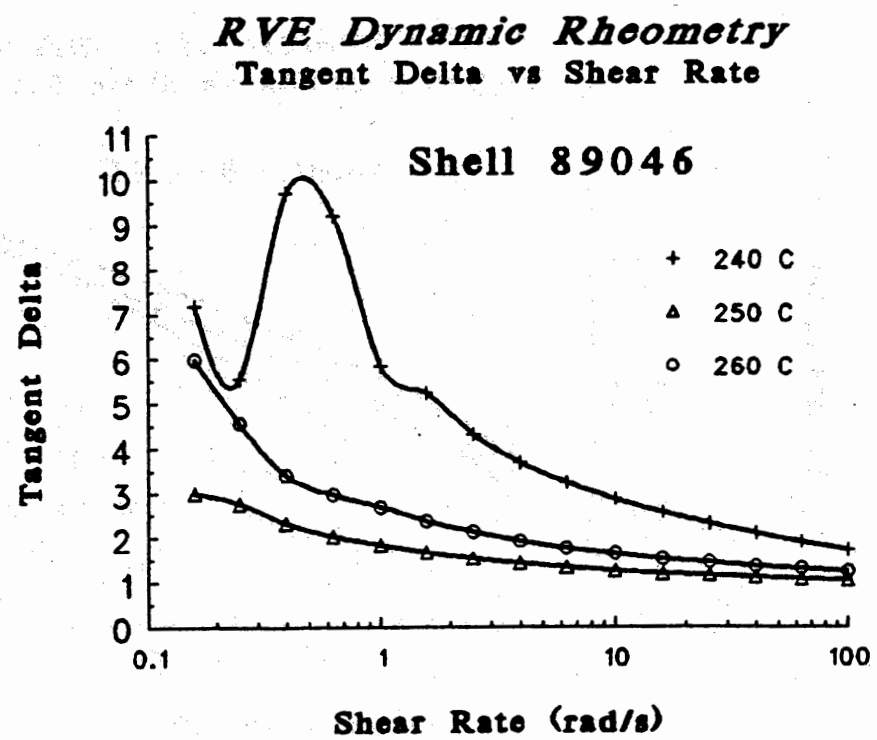

3.0 Tensile Properties of Unoriented Sheet

3.1 Introduction

The successful orientation of a polymer depends largely on the tensile properties as it relates to temperature. The tensile stress must be low, and the amount of elongation must be high at a particular temperature for successful orientation. For this reason, a study of tensile properties of extruded sheet as a function of temperature was completed.

3.2 Conclusion

- The orientation temperature for Shell 89046 should be ≈200°C or slightly greater.
- The orientation temperature for Shell 89022 should be ≈210°C or greater.
- Both Shell Resins, 89022 and 89044, show evidence of strain hardening, an important parameter for improved physical properties after orientation.

3.3 Experimental

Extruded sheet made from Shell 89022 and Shell 89046 resin were tested for tensile properties (uniaxial unconstrained orientation) under the following conditions:

ASTM D1708, Microtensile specimen
Instron Model TT-1101 with Instron Environmental Chamber
gagelenth = .876 in.
crosshead speed = 5 inch/minute
Strain Rate = 9.5% strain/second
Samples conditioned @ 23°C and 50% R.H.
Warmup at each temperature = 3 min.

3.4 Results and Discussion

Table IX through Table XI, and Figure 25 through Figure 28 present the tensile properties of Shell resins.

For successful orientation the yield peak should be small or not exist at a particular temperature. This signifies greater chain mobility with the absence of "neck-in". The yield stress should be 1000 psi or less and the ultimate elongation should be higher than the elongation necessary for a specific application.

This criteria is met at 200°C for Shell 89046, and 215°C for Shell 89022 as shown in Figure 25 and Figure 26.

In Figure 27 and Figure 28, at the same yield stress and elastic modulus, Shell 89022 would have a 10°C higher stretch temperature than Shell 89046.

Table IX Tensile Properties of Unoriented Sheet

material	temp (°C)	direction	thickness (mils)	Yield Stress (psi)	Yield Strain (%)	Ultimate Stress (psi)	Ultimate Strain (%)	Elastic Modulus (Kpsi)
89022	23	MD	14.6	9010	25.1	9340	282	128.0
			14.5	9090	26.7	8960	266	110.0
			15.0	9040	26.5	9730	210	143.0
			16.9	9210	27.8	9750	218	103.0
			16.9	8890	27.4	9180	271	98.2
		CD	14.6	9160	24.5	9160	224	136.0
			14.6	8880	24.8	8790	279	120.0
			14.6	9160	24.8	8970	303	137.0
			14.2	9280	25.1	9060	209	124.0
		mean	15.1	9080	25.9	9216	251	122.1
		std	1.0	138	1.3	336	36	15.7
89046	23	CD	22.8	7390	22.0	10900	369	83.3
			22.7	8450	22.3	7890	201	83.8
			22.6	8420	22.8	12300	405	117.0
		MD	22.9	8380	23.7	11900	370	92.7
			22.9	8410	24.3	11400	334	132.0
			23.0	8420	23.7	8740	223	109.0
			22.8	8770	24.8	12300	361	103.0
			22.5	8510	23.5	11500	375	139.0
		mean	22.8	8344	23.4	10866	330	107.5
		std	0.2	405	1.0	1658	75	20.9
89022	50	MD	14.4	9640	26.8	11330	371	87.8
			14.3	8060	24.3	9840	301	81.2
			14.5	9390	29.1	10290	284	76.3
		CD	14.6	7890	26.3	7840	268	55.9
			14.5	8480	25.1	9630	293	60.9
			14.5	9440	30.3	9150	217	83.8
		mean	14.5	8817	27.0	9680	289	74.3
		std	0.1	767	2.3	1165	50	13.0
89046	50	CD	22.0	8070	24.0	11080	419	64.8
			22.0	7290	24.0	11060	420	48.4
			22.2	7950	25.1	10910	404	60.3
		MD	22.4	8240	27.4	13250	450	65.4
			22.8	7150	22.8	11730	435	50.1
			22.5	8150	24.5	12980	450	66.2
		mean	22.3	7808	24.6	11835	430	59.2
		std	0.3	468	1.6	1034	19	8.0

Table X Tensile Properties of Unoriented Sheet - *continued*

material	temp (C)	direction	thickness (mils)	Yield Stress (psi)	Yield Strain (%)	Ultimate Stress (psi)	Ultimate Strain (%)	Elastic Modulus (Kpsi)
89022	100	CD	14.3	7050	26.2	9400	428	66.4
			14.3	7240	26.0	6580	211	61.8
			14.1	6590	26.9	6750	291	54.0
			14.3	6280	25.6	8510	403	53.8
		MD	14.9	7053	26.3	7340	270	67.6
			15.0	6560	26.0	9930	439	52.2
			14.2	6650	27.9	6480	268	52.0
			14.9	6530	27.5	9510	393	53.6
		mean	14.5	6744	26.6	8063	338	57.7
		std	0.4	330	0.8	1440	87	6.5
89046	100	CD	21.8	5720	21.9	5810	320	45.2
			21.7	6070	22.5	7930	410	61.0
			21.7	5790	22.8	8910	479	54.0
		MD	21.4	5710	22.8	6750	336	43.1
			21.8	5690	24.5	7790	387	44.2
			21.6	5830	23.5	8620	438	49.4
		mean	21.7	5802	23.0	7635	395	49.5
		std	0.2	142	0.9	1168	60	6.9
89022	150	CD	14.1	4510	23.4	8060	645	43.9
			14.3	4520	23.9	6620	492	42.7
			14.0	4560	23.4	9052	656	47.5
		MD	14.7	4600	23.4	8640	576	40.4
			14.3	4670	22.8	5120	471	40.7
			14.0	4560	24.0	9260	631	40.0
		mean	14.2	4570	23.5	7792	579	42.5
		std	0.3	59	0.4	1615	80	2.9
89046	150	MD	22.3	3860	23.7	8990	> 690	
			22.7	3830	22.3	8830	> 690	38.7
			22.8	3790	22.8	8910	> 690	44.9
		CD	22.6	3860	21.1	8380	> 690	42.8
			22.7	3820	21.1	7950	> 690	51.4
			22.8	3780	21.7	8300	> 690	41.1
		mean	22.7	3823	22.1	8560		43.8
		std	0.2	34	1.0	413		4.8

Table XI Tensile Properties of Unoriented Sheet - *continued*

material	temp (C)	direction	thickness (mils)	Yield Stress (psi)	Yield Strain (%)	Ultimate Stress (psi)	Ultimate Strain (%)	Elastic Modulus (Kpsi)
89022	170	MD	14.1	3750	24.5	8440	> 690	42.5
			14.4	3750	23.8	8360	> 690	37.2
			14.1	3890	23.1	8440	> 690	37.4
		mean	14.2	3797	23.8	8413		39.0
		std	0.2	81	0.7	46		3.0
89046	170	MD	22.2	2990	20.8	6740	> 690	33.8
			22.2	2960	19.4	6870	> 690	35.0
			22.0	3090	21.7	7000	> 690	24.9
		mean	22.1	3013	20.6	6870		31.2
		std	0.1	68	1.2	130		5.5
89022	185	MD	14.2	2860	20.3	6480	> 690	24.9
			14.1	2790	20.0	6260	> 690	36.6
			15.0	2780	20.2	6560	> 690	28.5
		mean	14.4	2810	20.2	6433		30.0
		std	0.5	44	0.2	155		6.0
89046	185	MD	22.4	2280	18.0	5170	> 690	31.7
			22.7	2120	17.7	4920	> 690	29.6
			22.4	2150	18.8	4890	> 690	27.6
		mean	22.5	2183	18.2	4993		29.6
		std	0.2	85	0.6	154		2.1
89022	200	MD	15.0	1500	15.7	3990	> 690	26.2
			14.5	1600	16.6	3840	> 690	38.9
			14.2	1580	15.1	3840	> 690	27.4
		mean	14.6	1560	15.8	3890		30.8
		std	0.4	53	0.8	87		7.0
89046	200	MD	23.7	1070	12.6	2520	> 690	20.3
			23.0	967	12.6	2200	> 690	16.7
			23.0	990	12.5	2230	> 690	20.1
		mean	23.2	1009	12.6	2317		19.0
		std	0.4	54	0.1	177		2.0
89022	215	MD	15.0	774	11.4	1760	> 690	16.7
			16.0	715	10.6	1620	> 690	9.4
			14.2	757	12.8	1730	> 690	12.3
		mean	15.1	749	11.6	1703		12.8
		std	0.9	30	1.1	74		3.7
89046	215	MD	22.7	-	-	125	55	0.2
			22.5	-	-	109	79	0.2
		mean	22.6			117	67	0.2

Figure 25 **Tensile Properties of Shell 89022**

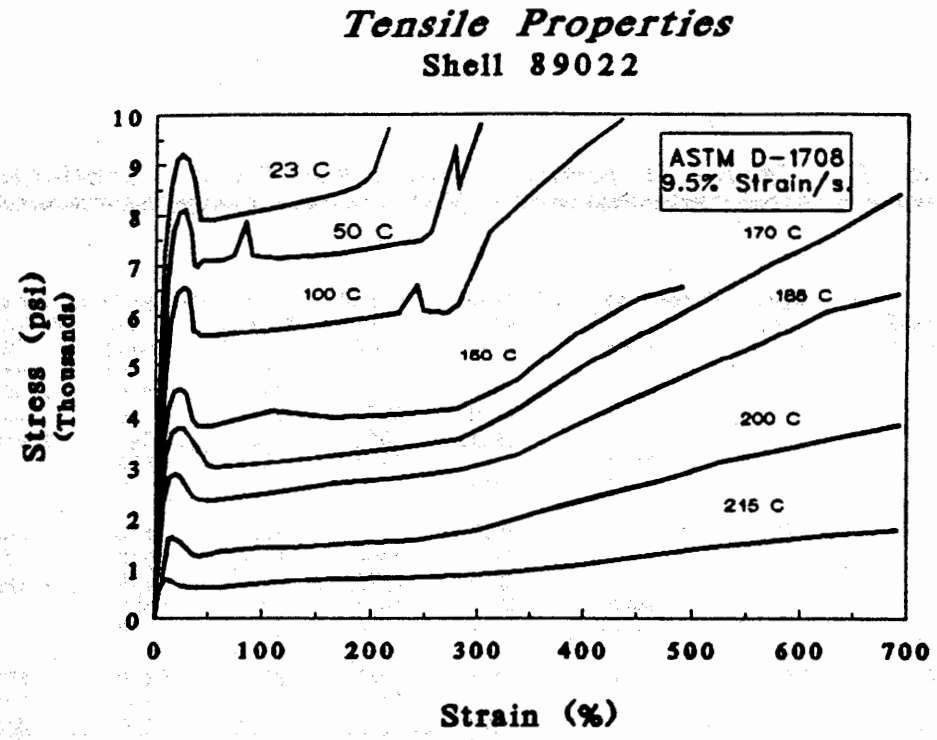

Figure 26 **Tensile Properties of Shell 89046**

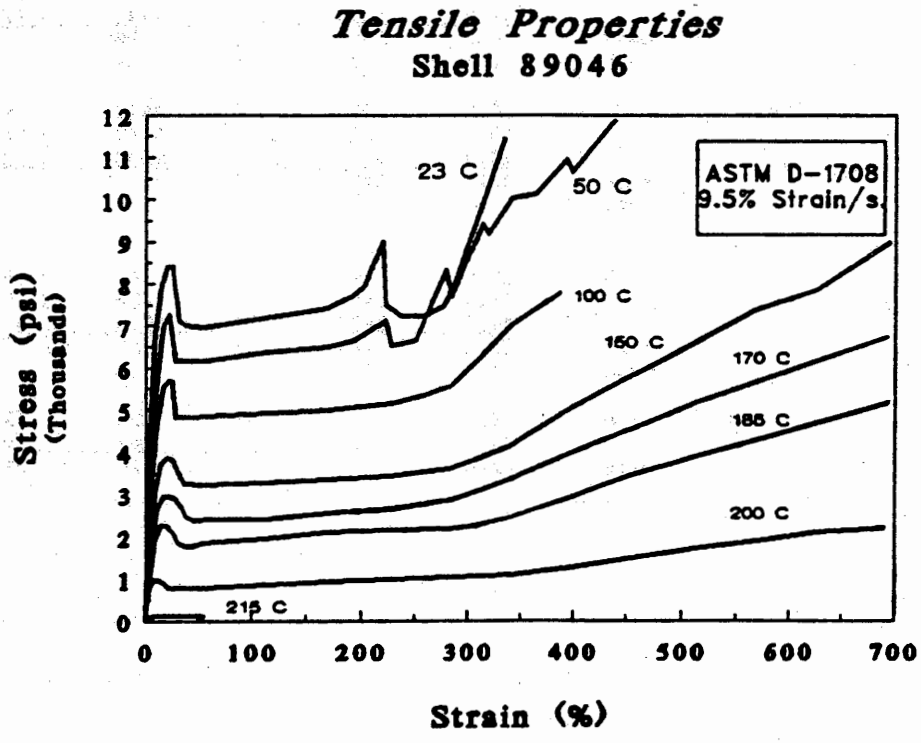

Tensile Properties of Unoriented Sheet

Figure 27 **Yield Stress vs Temperature**

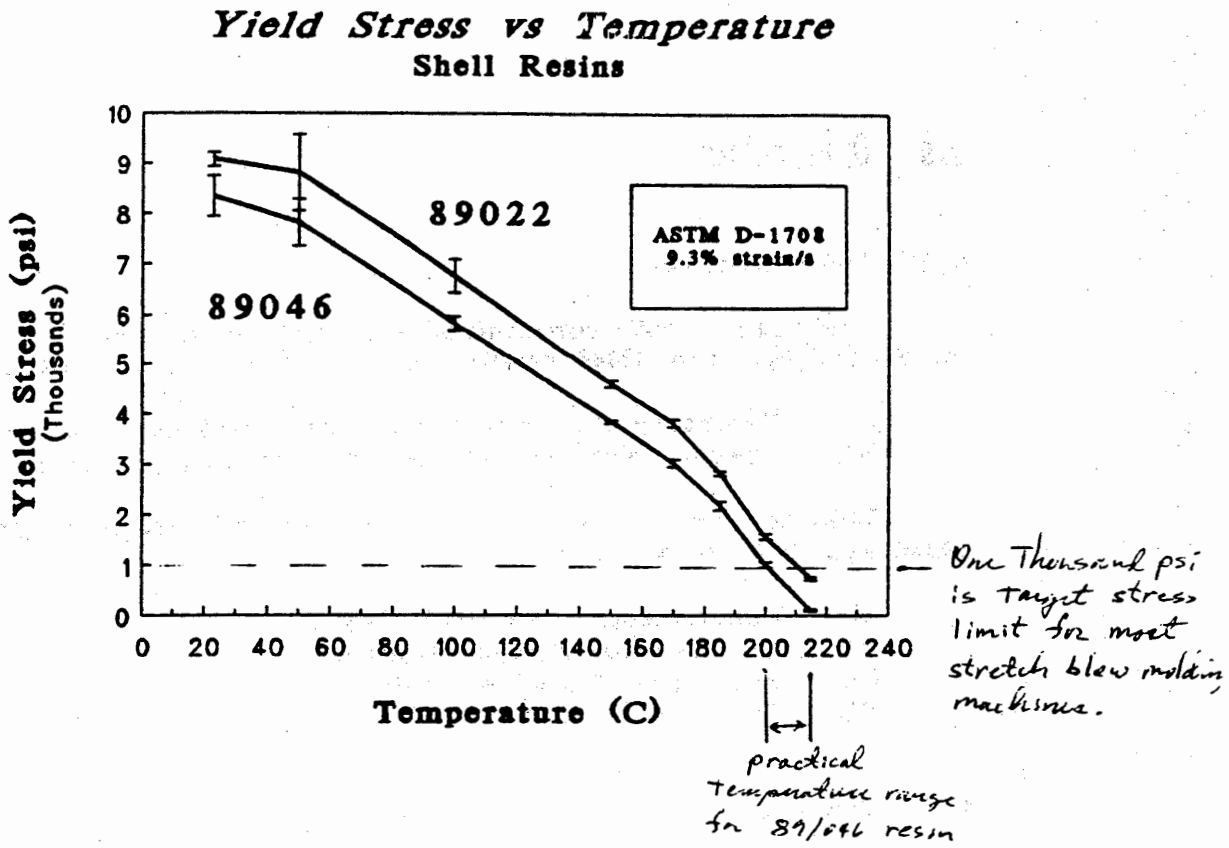

Figure 28 **Elastic Modulus vs Temperature**

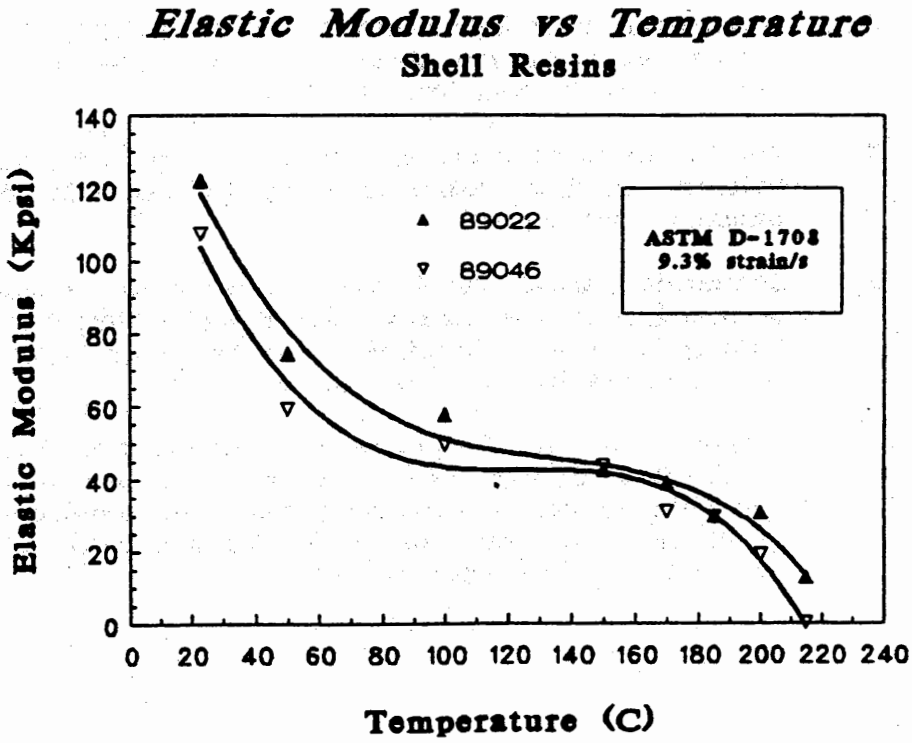

4.0 Orientation

4.1 Introduction

Orientation, both constrained uniaxial and biaxial, has been completed for Shell 89022 and 89046 resins. The objective of orientation is two-fold:

a). Determine the orientation characteristics of the film.
b). Prepare oriented samples for physical property measurements.

This section discusses the orientation characteristics of 89022 and 89046 resins as they relate to:

a). Constrained Uniaxial extension.
b). Simultaneous Biaxial extension.
c). Sequential Biaxial extension.
d). Strain Hardening.

4.2 Conclusions

- For good, even uniaxial orientation of Shell 89046, a temperature of 200°C to 210°C is best. Strain hardening occurs at 5.5 extension ratio (203°C).

- Good, even, uniaxial orientation of Shell 89022, occurs at 10°C higher temperature and strain hardening occurs at lower extension ratio than Shell 89046.

- For biaxial orientation of both Shell resins, it will be necessary to raise the temperature of orientation slightly higher than uniaxial orientation.

- Sequential biaxial orientation, compared to simultaneous biaxial orientation, should improve the material distribution in the film. This is because no yield point during sequential orientation was recorded in the stress-strain curve.

- Strain hardening, the increase of stress after the yield point, is essential for improved physical properties in oriented film. The onset of strain hardening has been modeled to linear equations which could be useful for prediction of strain hardening during orientation.

4.3 Experimental

Shell Resin 89022 and 89046 from extruded sheet were conditioned at 50% ± 2% R.H. and 72° ± 1°F before orientation.

The following machine and test conditions were used:

Long Extensional Tester (L.E.T.)
Gage Length: 2 inch x 2 inch.
Width: 2.44 inch.
Mode: Constrained Uniaxial, Simultaneous and Sequential Biaxial

Strain is calculated by the extension ratio.

$$\lambda = \frac{L_f}{L_o}$$

λ = extension ratio
L_f = Final Length
L_o = Gage Length

Stress, τ, is calculated as the engineering stress based on the original cross-sectional area of the film.

$$\tau = \frac{Load}{Original\ Area}$$

4.4 Results and Discussion

4.41 Temperature and Constrained Uniaxial Orientation

The results of uniaxial orientation are shown graphically in Figure 29 to Figure 31. It is important to prevent a yield stress peak from occurring in the stress-strain curve because a large peak signifies uneven stretching. It is also desirable for the stress to rise at a strain greater than the yield peak (strain hardening) for improved physical properties.

The effect of temperature on uniaxial orientation of Shell 89046 is shown in Figure 29. A temperature of 203°C is necessary to eliminate the yield stress peak and provide optimum extension ratio. Strain hardening, at 203°C occurs at 5.5 extension ratio.

Figure 29 **Uniaxial Orientation of Shell 89046**

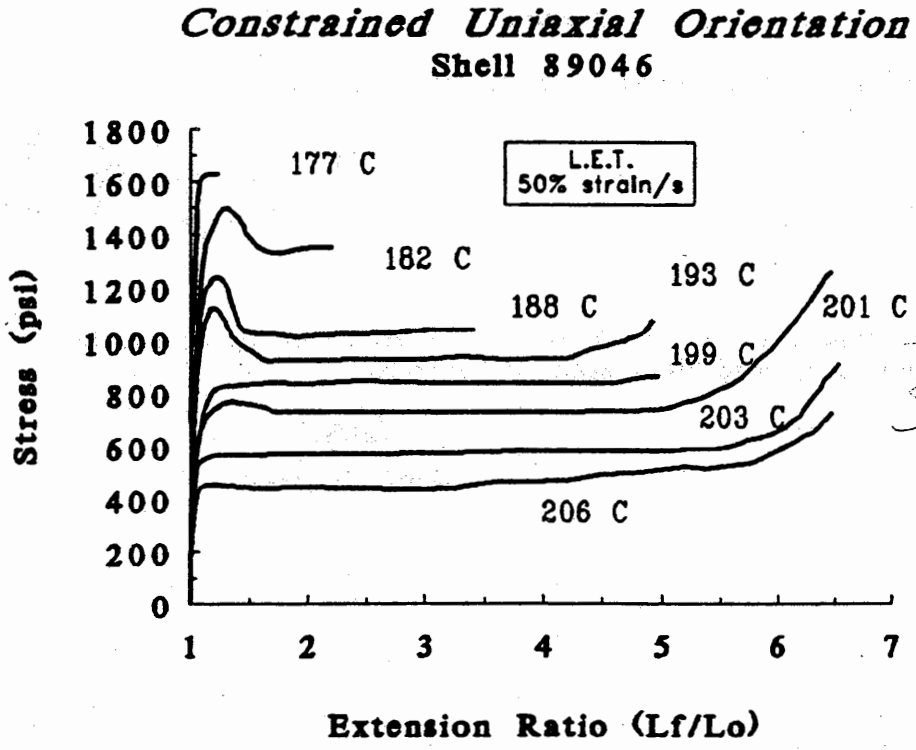

Orientation of Shell 89022, shown in Figure 30, has an optimal temperature approximately 10°C higher than Shell 89046. The optimal temperature for orientation is 210°C to 215°C. Strain hardening for uniaxial orientation occurs between 4.75 and 5.0 extension ratio.

Figure 30 Uniaxial Orientation of Shell 89022

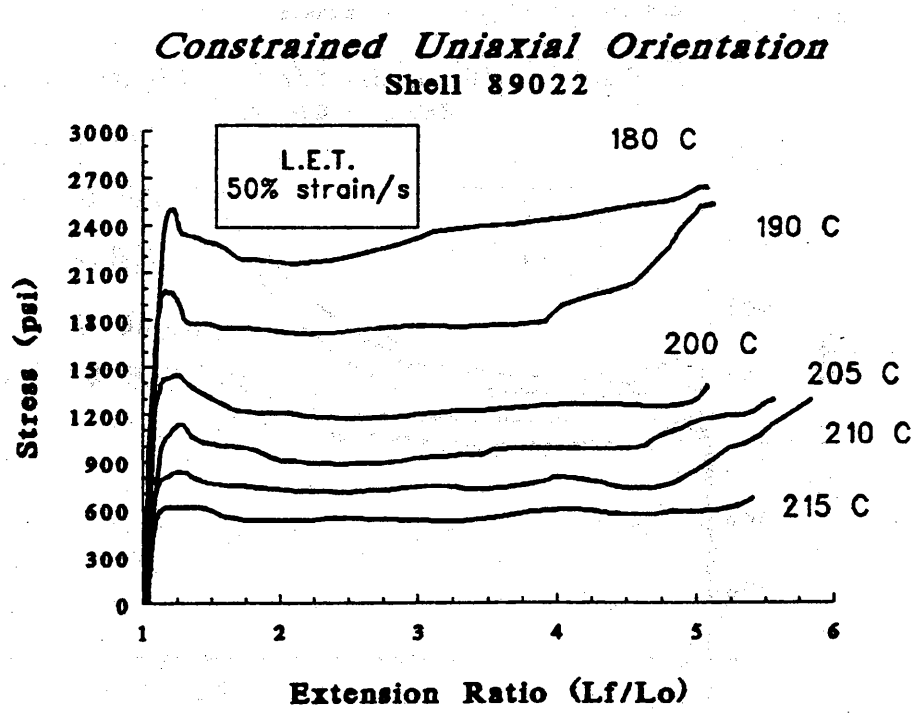

with so little strain hardening it is very difficult to avoid tearing the parison.

4.42 Strain Rate and Constrained Uniaxial Orientation

As shown in Figure 31, changing strain rate for Shell 89046 is much like changing temperatures. Going to higher strain rate has the same effect as going to lower temperatures. For better orientation at high strain rates, the temperature should be increased compared to lower strain rates.

Figure 31 **Effect of Strain Rate on Uniaxial Orientation**

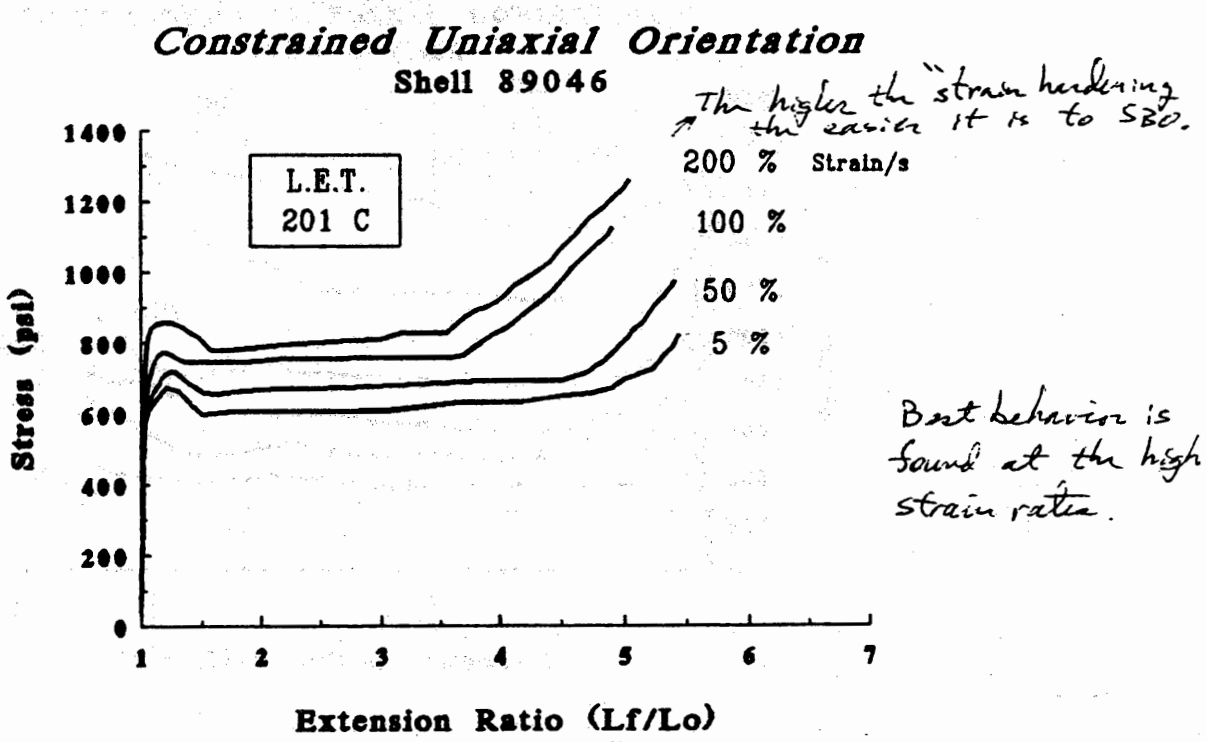

4.43 Simultaneous Biaxial Orientation

The simultaneous biaxial orientation (both x and y axis are stretched at the same time) stress and strain properties were determined for Shell 89022 and Shell 89046.

As shown in Figure 31 for Shell 89046, the strain hardening parameter is met at an earlier extension ration than occurred with uniaxial orientation. This will be a benefit for physical properties.

The greater presence of a yield peak during biaxial orientation suggests higher temperatures are required than during uniaxial orientation.

Figure 32 **Simultaneous Biaxial Orientation of Shell 89046**

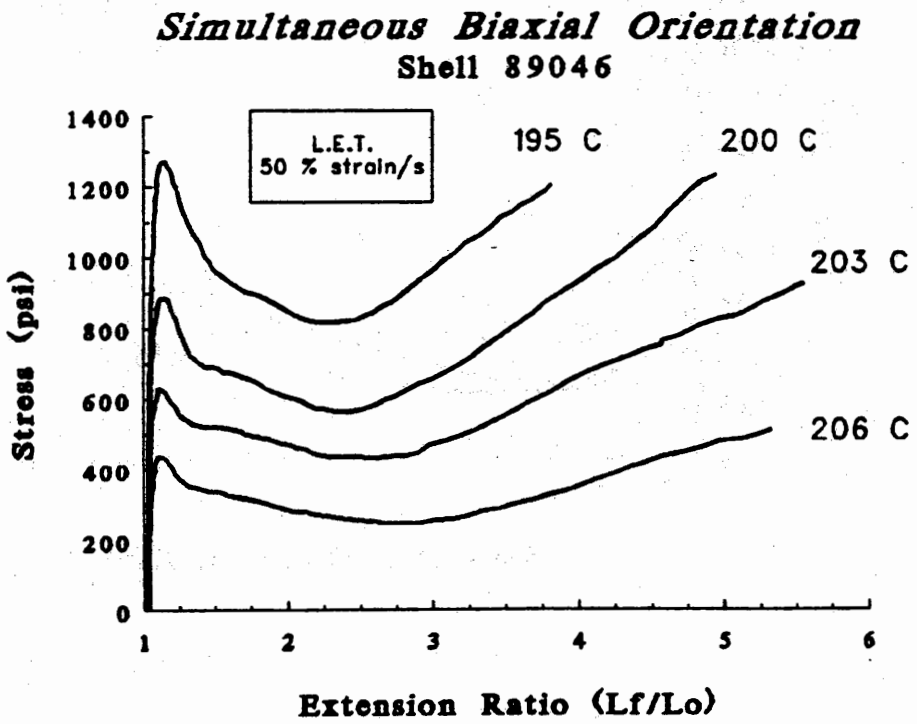

Simultaneous biaxial orientation of Shell 89022 is shown in Figure 32. Like Shell 89046, Shell 89022 strain hardens at a lower extension ratio and requires a higher temperature of orientation than during uniaxial orientation.

Figure 33 **Simultaneous Biaxial Orientation of Shell 89022**

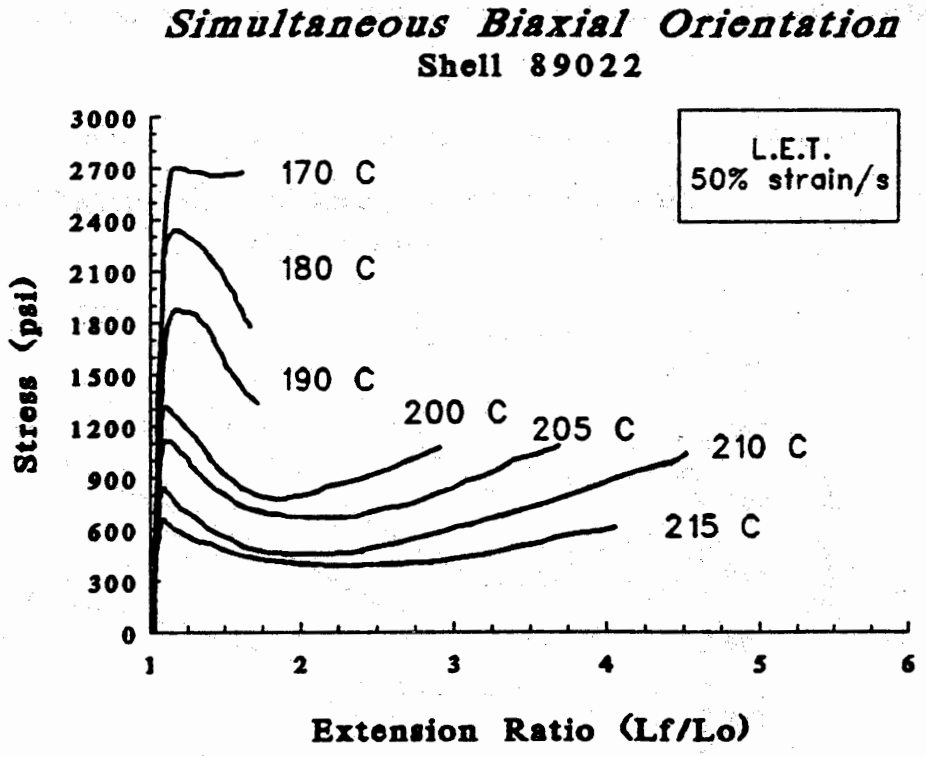

Simultaneous biaxial orientation at a higher strain rate is shown in Figure 34 at 200% strain/second. In comparison to a strain rate of 50%/second, the orientation stress is higher and the break point is at shorter extension ratios.

Figure 34 **Biaxial Orientation of Shell 89022 at Higher Strain Rates**

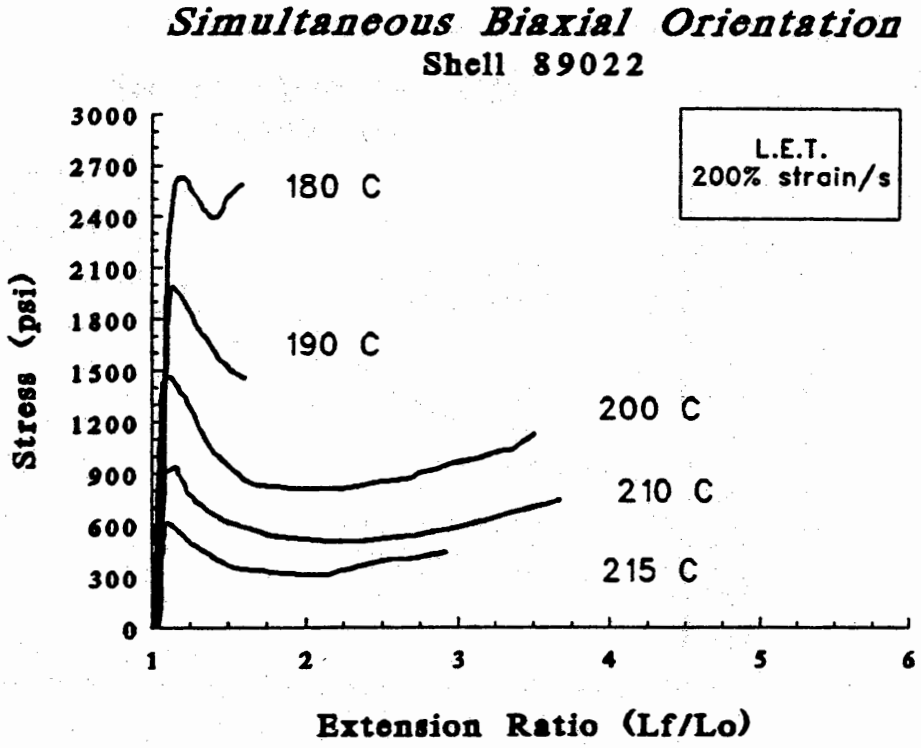

Sequential biaxial orientation (first stretch y axis uniaxially then stretch the x axis) of Shell 89022 is shown graphically in Figure 35. This plot is a comparison with simultaneous orientation and shows dramatic differences in stress strain behavior.

The major difference in the stress-strain curve is the absence of the yield peak for sequential orientation. This can result in more even stretching, especially at lower extension ratios.

Figure 35 **Sequential Biaxial Orientation of Shell 89022**

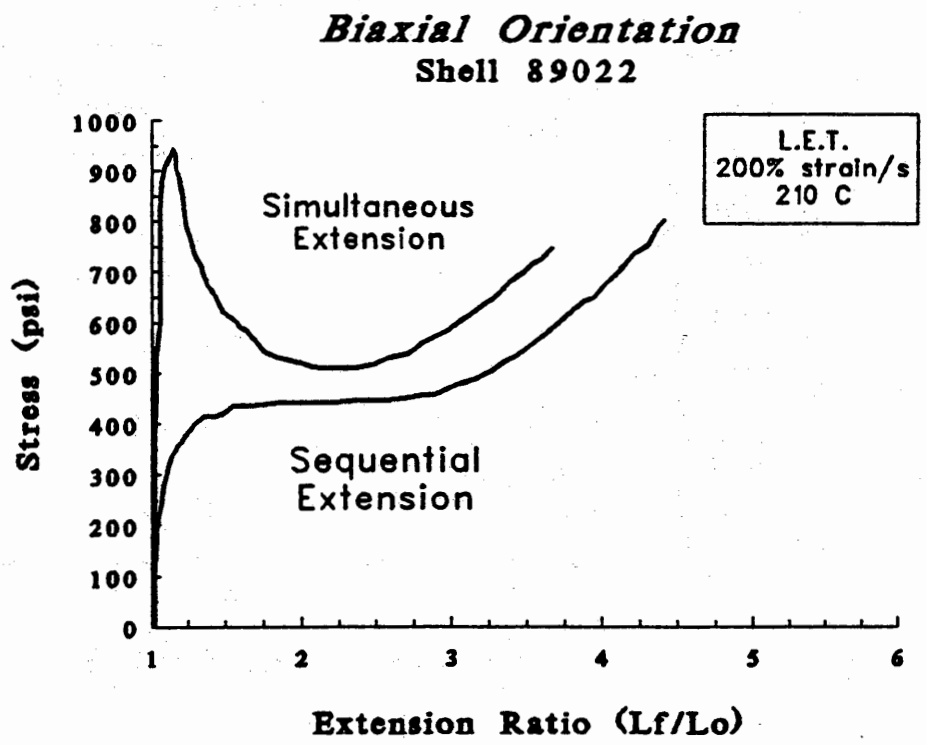

Conclusion. stretch longitudinally first, then apply blow air to orient in hoop direction of container. This minimizes draw band formation + gives uniform drawing behavior.

Sequential Biaxial Orientation of Shell 89046 is presented in Figure 36. This data is a comparison of Simultaneous versus Sequential stress-strain curves. Stretched 2.5x in longitudinal direction, then 4x in transverse direction.

Like the sequential stress-strain curves of Shell 89022, the yield point of the orientation stress disappears. The result will be more even stretching of sequentially oriented film.

Figure 36 **Sequential Biaxial Orientation of Shell 89046**

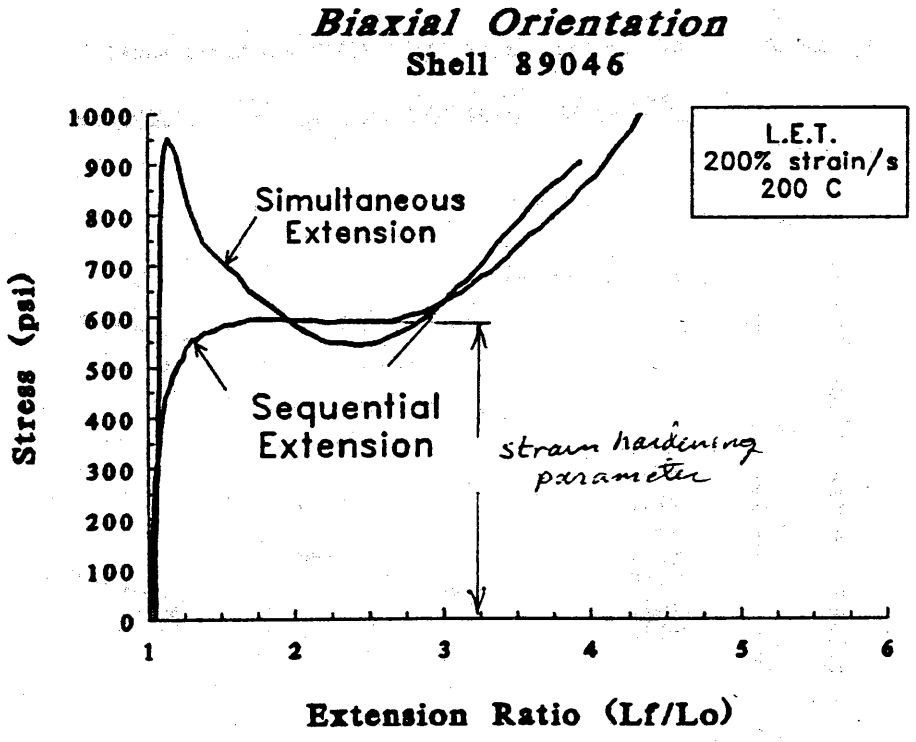

4.43 Strain Hardening

As mentioned before, strain hardening is a desired property. Strain hardening is the increase of stress with increase in strain, that occurs past the yield point. Strain induced crystallization in responsible for strain hardening and can result in improved physical properties.

The critical extension ratio is defined as the extension ratio, under a certain set of orientation conditions, that strain hardening is induced. When films are oriented above the critical extension ratio, improved physical properties are the result.

Strain hardening and the critical extension ratio are predictable properties for Shell 89022 and Shell 89046. As shown in Figure 37 the critical extension ratio is linear with respect to temperature at a strain rate of 50% strain/sec.

Figure 37 **Strain Harding of Shell 89022 and Shell 89046**

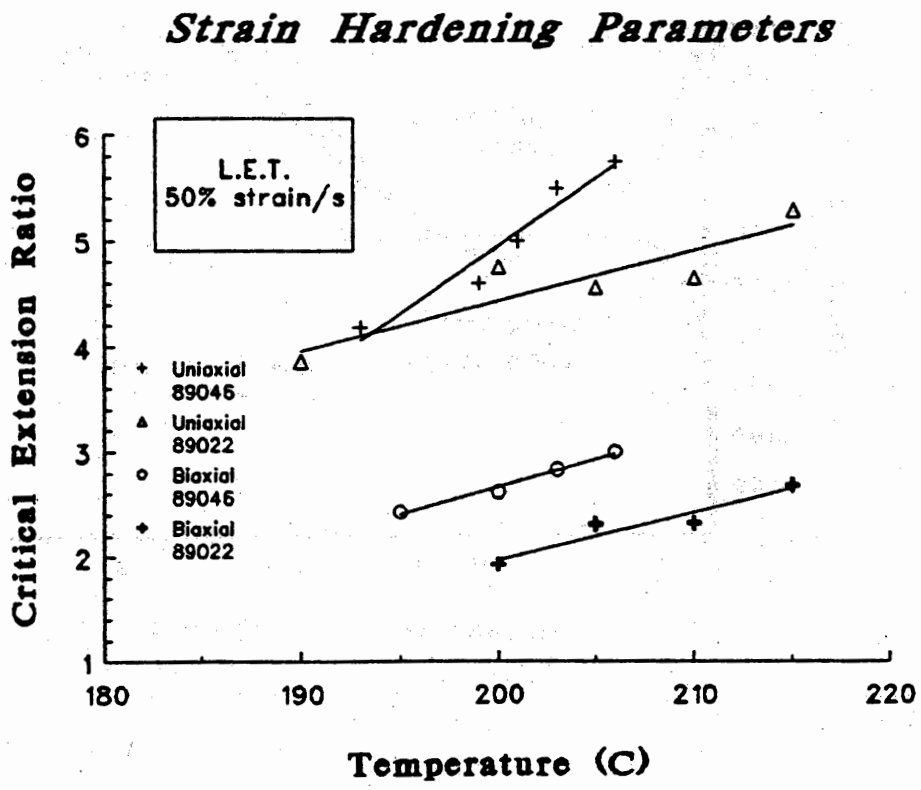

Table XII lists the linear least squares constants, according to the following equation, under uniaxial or biaxial orientation of Shell 89022 and 89046.

$$\lambda_c = A + B \times Temp(^\circ C)$$

λ_c = critical extension ratio
A = intercept
B = slope
Temp = temperature

Table XII Onset of Strain Hardening

Resin	Orientation Mode	Intercept (λ)	slope (λ/°C)
89022	Uniaxial	-5.1	0.048
	Biaxial	-7.07	0.045
89046	Uniaxial	-20.5	0.124
	Biaxial	-7.82	0.052

5.0 Tensile Properties of Oriented Film

5.1 Introduction

The physical property benefits that result from orientation of Shell 89022 and 89046 material can be determined by testing the oriented film for tensile properties. As the Ultimate Stress, Ultimate Strain, and Elastic Modulus is seen to increase, then the orientation benefit will be increased toughness and flexibility.

5.2 Experimental

Shell 89022 and 89046 films, oriented under various conditions were tested for room temperature tensile properties under the following conditions:

Instron Tensile Tester TM-1101
ASTM D-1708 Micro-Tensile
Crosshead speed: .5 inch/minute
Strain Rate: 9.5% strain/second
Temperature: 23°C

5.3 Conclusions

- Tensile Properties of oriented Shell resins, 89022 and 89046, are improved compared to unoriented Shell resins.
- Overall, equal biaxial orientation (i.e. 2 x 2, 3 x 3, 4 x 4 extension ratio) results in the best tensile properties.
- Unbalanced orientation results in good properties in one direction only. The tensile properties in both directions can be unbalanced.

5.4 Results and Discussion

Results are presented in Table XIII for Shell 89022 and Table XIV for Shell 89046, which lists mean and standard deviation (σ) values for machine direction (MD) or the cross direction (CD) of the extruded film. Orientation is listed as extension ratio. The first number of an oriented film's extension ratio refers to the machine direction of the film (i.e. 2 x 3 where the machine direction was oriented 2x times the original length. These tables show ultimate stress and elastic modulus of oriented films has increased and the ultimate strain has decreased compared to the unoriented film.

Figure 38 and Figure 39 show equal biaxial orientation of Shell 89022 and Shell 89046 respectively. Generally increased orientation results in increased stiffness and strength.

Figure 40 shows Shell 89022 with increased levels of orientation in the cross-direction but measured for tensile properties in the extruded machine direction. The tensile properties in the machine direction decrease as the orientation in the cross-direction is increased.

Figure 41 shows the same Shell 89022 films, with increasing orientation level in the extruded machine direction and measured for tensile properties in the machine direction. In this case, the tensile properties have increased. However, the tensile properties of the film in each direction is very unbalanced.

Tensile Properties of Oriented Film

Table XIII Tensile Properties of Oriented Shell 89022

Oriented by L.E.T. @ 210°C ASTM D-1708					
orientation	**direction**	**thickness (mils)**	**Ultimate Stress (psi)**	**Ultimate Strain (%)**	**Elastic Modulus (Kpsi)**
unoriented	md	15.6	9390	249	116
	σ	1.2	345	33	19
	cd	14.5	9000	237	127
	σ	0.2	190	37	8.3
2 x 2	md	3.7	20000	108	243
	σ	0.2	2700	3	40
	cd	4.7	17400	122	196
	σ	0.2	1010	26	23
2 x 3	md	3.3	14900	113	194
	σ	0.4	1720	20	16
	cd	2.6	26000	41	247
	σ	0.1	7790	14	9
2 x 5	md	2.1	10900	100	158
	σ	0.2	980	16	11
	cd	1.9	18100	13	265
	σ	0.1	10800	8	41
3 x 3	md	1.9	23900	61	194
	σ	0.1	656	4	17
3 x 4	md	1.7	20500	73	165
	σ	0.1	2500	16	22
	cd	1.6	22700	30	208
	σ	0.2	9154	17	17
3 x 5	md	1.5	18400	66	156
	σ	0.1	777	6	29
	cd	1.4	24900	21	212
	σ	0.1	212	5	21
4 x 4	md	1.2	19900	24	192
	σ	0	4780	6	39
	cd	1.6	21800	41	167
	σ	0.3	3700	7	35

Table XIV Tensile Properties of Oriented Shell 89046

ASTM D-1708 Oriented by L.E.T.					
Orientation	**stats**	**thickness**	**Ultimate Stress (psi)**	**Ultimate strain (%)**	**Elastic Modulus (Kpsi)**
Unoriented	MD	22.8	11200	332	115
	σ	0.2	1400	63	20
	CD	22.7	10400	325	95
	σ	0.1	2250	109	19
3 x 3 200°C		3.2	22400	81	182
	σ	0.4	1320	2	46
3 x 3 203°C		3.2	19500	67	212
	σ	0.2	3100	25	33
4 x 4 200°C		1.8	23400	33	294
	σ	0.1	3670	8	77
4 x 4 203°C		1.6	24000	37	253
	σ	0.1	611	6	73

Figure 38 Tensile properties of Equal Biaxial Oriented Shell 89022

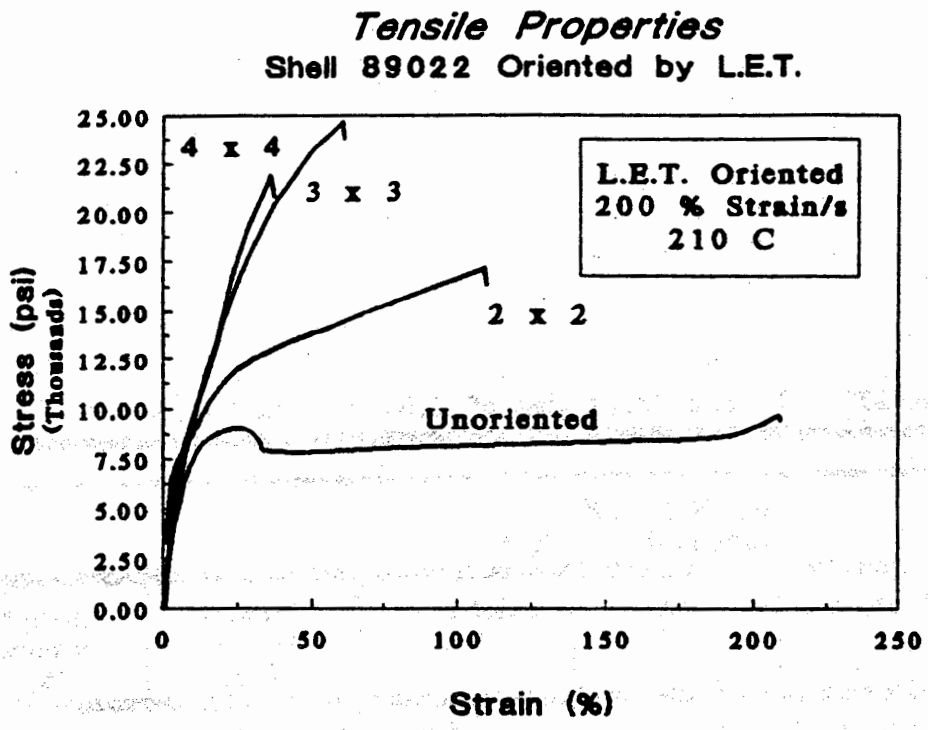

Figure 39 Tensile Properties of Equal Biaxial Oriented Shell 89046

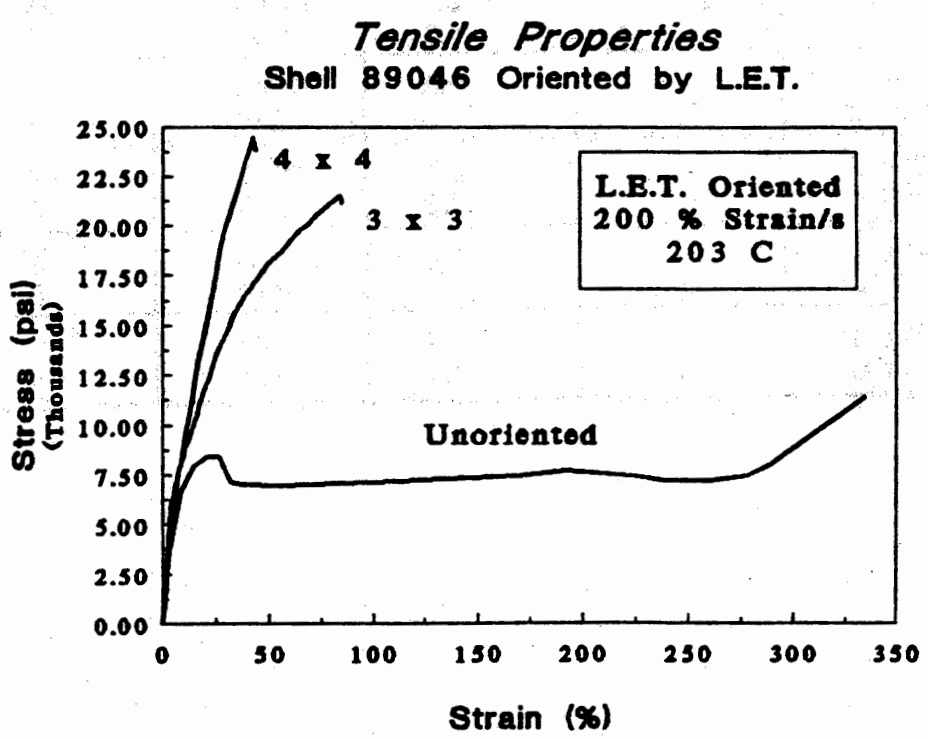

Figure 40 Tensile Properties of Oriented Shell 89022 in M.D.

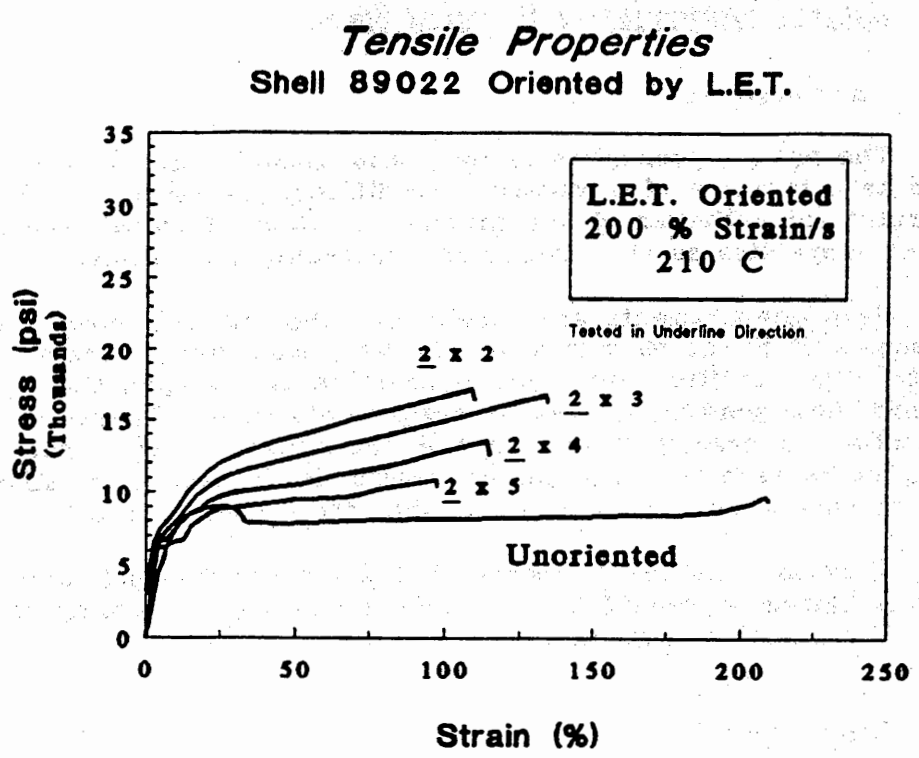

Figure 41 Tensile Properties of Shell 89022 in C.D.

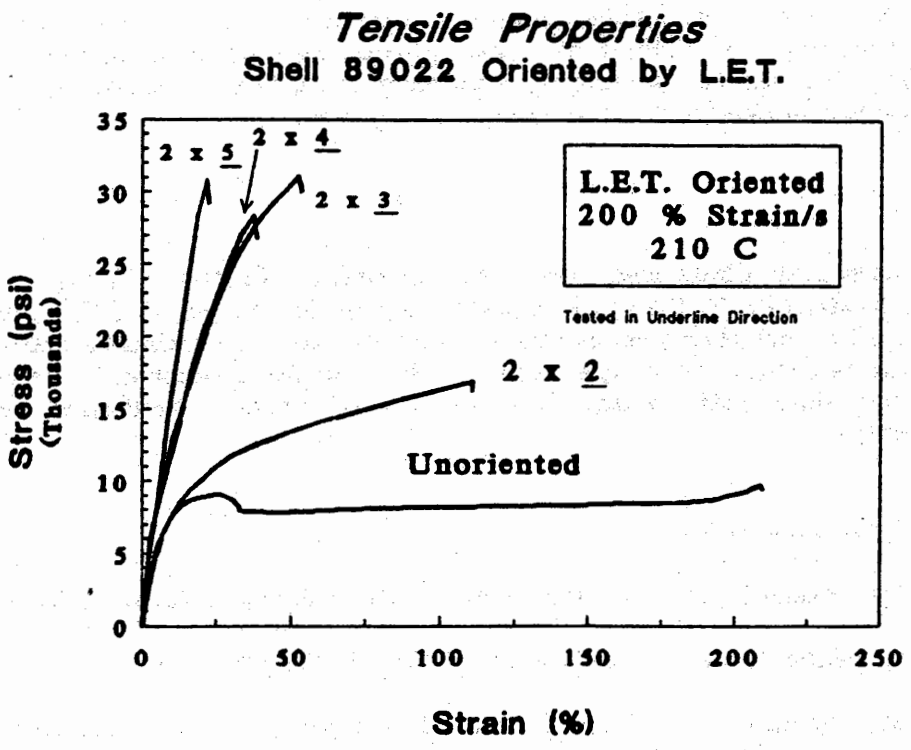

6.0 Optical Properties of Oriented Sheet

6.1 Introduction

The optical properties of haze and gloss were determined for material 89046 as a function of orientation conditions. Since haze and gloss are important for esthetics of the finished product, it is important to know the optical properties as they relate to processing conditions.

Haze measurements are simple, but the interpretation is complicated. In essence it is the measurement of light scattering, therefore it is caused by structural entities which are present in the sample, that is, crystalline systems, homogeneity, as well as sample thickness. Therefore, the effect of orientation on haze in done with the understanding that there is a reduction in haze with decreasing sample thickness. For esthetics, the percent haze should be low as possible for a clear product.

Gloss is a texture property that gives the product luster or shine. Gloss is extremely sensitive to surface properties. In many cases, high gloss is desired for esthetics.

6.2 Experimental

Haze

Percent haze was measured according to the ASTM procedure D 1003 using a Gardner Pivotable-Sphere Hazemeter. The haze measured using this procedure is defined as "that percentage of transmitted light which, in passing through the specimen, deviates from the incident collimated beams by forward scattering more that 2.5 degrees."

Gloss

Specular gloss was measured according to the ASTM procedure D 523 using a Gardner Multi-Angle Glossmeter at an angle of 60°. The gloss measured using this procedure is defined as "the relative luminous reflectance factor on a specimen in the mirror direction." Measurements of gloss correlate with visual observations of surface brilliance made at the same angle.

6.3 Conclusions

- In general, the percent haze is decreasing with orientation.
- A reduced haze appears at a planar strain of 9.
- It appears that at high extension ratios, the percent haze does not change significantly with oven temperature.
- A high level of gloss is achieved at a planar strain of 15.

6.4 Results and Discussion

For comparison purposes, Table XV gives the percent haze as a function of oven temperature and orientation level for Shell 89046, oriented at 200% strain/second. In general, the percent haze is decreasing with orientation level.

Planar strain is the product of the extension ratios in the machine direction and the cross direction. It appears that at high extension ratios, the percent haze does not change significantly with oven temperature and that a reduced haze appears at a planar strain of 9.

Table XV % Haze for Shell 89046

Stretch Ratio	Stretch Temperature			
	195°C	200°C	203°C	206°C
1 x 2	-	90	66	83
1 x 3	32	71	34	65
1 x 4	20	29	24	43
1 x 5	-	18	19	x
1 x 5 Reheat > 12°	-	-	38	-
1 x 6	-	15	-	-
2 x 2	21	39	61	50
2 x 3	19	26	36	24
2 x 4	-	12	20	18
2 x 5	-	10	13	x41
3 x 3	7	14	18	x19
3 x 4	x9	7	12	-
3 x 5	-	4	7	-
4 x 4	x7	3	6	-

- No Sample
X Sample broke during stretching

Gloss is reported in Table XVI. From the data, a high level of gloss is achieved at a planar strain of 15 or above. The temperature effects on gloss are negligible.

Table XVI Gloss @ 60°, Shell 89046

Stretch Ratio	Stretch Temperature			
	195°C	200°C	203°C	206°C
1 x 2	-	6	7	7
1 x 3	10	6	8	7
1 x 4	7	8	10	10
1 x 5	-	15	11	x
1 x 5 Reheat > 12°	-	-	8	-
1 x 6	-	3	-	-
2 x 2	4	5	4	7
2 x 3	8	12	8	10
2 x 4	-	13	6	8
2 x 5	-	8	7	x
3 x 3	4	7	6	x8
3 x 4	x10	17	8	-
3 x 5	-	44	53	-
4 x 4	x13	44	43	-

- No Sample
X Sample broke during stretching

7.0 IR Heating Characteristics

7.1 Introduction

The Infra-Red transmission through Shell 89046 Resin was obtained over a wide range of wave lengths for a 1.8 mil thick film sample. The results were compiled to extract data for the numerical solution to the IR heating system normally used in the PET beverage bottle blow molding process. To this end, the absorption coefficient as a function of the IR wave length for the material was obtained, so that IR radiation power penetration can be calculated.

7.2 Conclusion

- During IR heating in a PET type blow molding process, most of the heat will be absorbed in the surface region and very little radiation heat will reach the interior of the parison. Modifications to the heater system and heating procedure are required.

7.3 Results and Discussion

Figure 42 represents the relation between the percent transmission of IR radiation power through a 1 mm thick Shell resin sample as a function of wave length. For comparison purposes, the transmission spectra of PET is shown along with the IR radiation spectrum from a heater at a temperature of 2400°K.

From the figure, it is seen that the maximum penetration of IR radiation takes place in the range of wave lengths between 1.5 to 2.2 microns, and that in this range only about 20% of the IR radiation can penetrate to a depth of 1 mm for Shell resin. For PET, 95% of the IR radiation can penetrate to a depth of 1 mm. This means during the IR heating process of Shell resin, most of the heat would be absorbed in the surface region and very little radiative heat would reach the interior or the inside surface of a typical parison having a 4 mm thick wall.

Figure 42 Transmission of IR Radiation

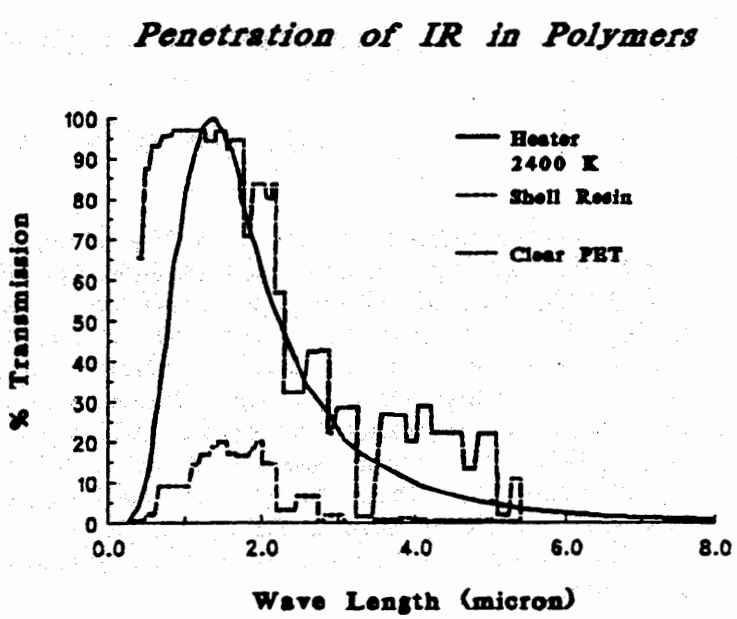

IR Heating Characteristics

The IR power distribution in a parison wall can be calculated from the IR radiation spectrum of the heater and the IR absorption coefficient distribution of the material. To be more specific, assume the parison wall thickness is 4 mm. and the IR heater temperature is 2450°K. Under a typical high intensity heating system, the power distribution would look like the "Shell" curve in Figure 43. For comparison, the IR heating power distributions for "Clear PET" and "Amber PET" are also shown in the figure. As can be seen by comparing these curves, the Shell resin tends to heat on the outside surface much more than other materials. Therefore, in order to heat the parison made from Shell resin properly without excessively over heating the surface region, special precautions must be taken to remove or to reduce the surface heat concentration during the heating operation. One alternative is to reduce the intensity of the IR heating source, and to rely heavily on the heat conduction to diffuse the heat from the outside surface towards the inside.

Figure 43 **IR Heating Power Penetration**

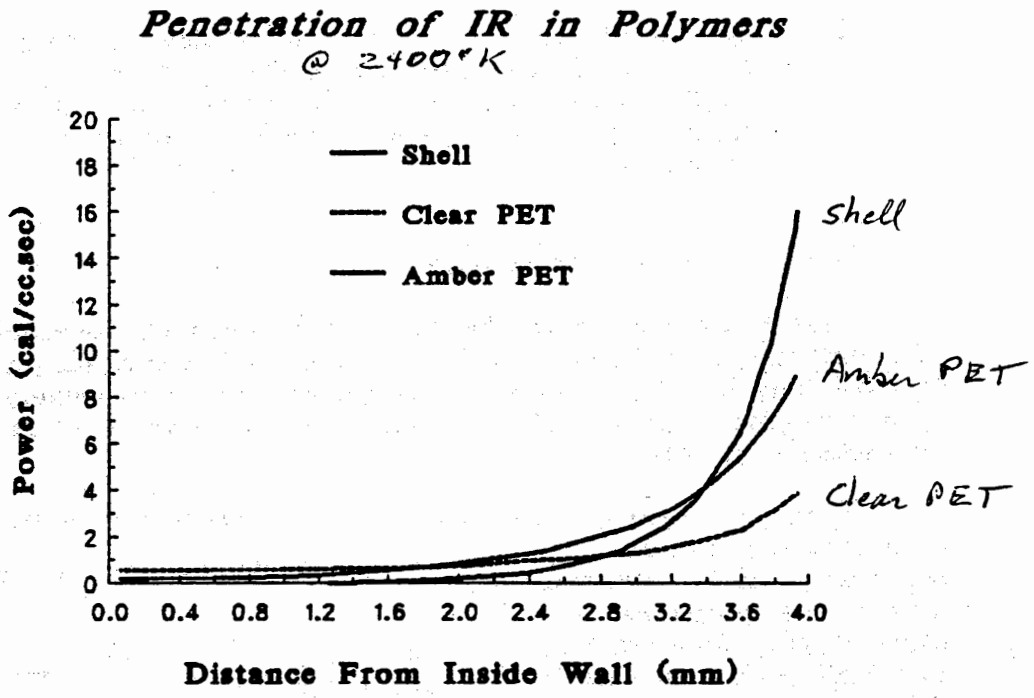

One unsettled question in the evaluation of the IR absorption coefficient is the possible errors involved in using such a thin specimen (1.8 mils). The IR absorption coefficients for the Eastman PET and for the amber PET were evaluated from an actual parison with about 4 mm thick walls. However, we are fairly confident in the validity of the results based on our extended period of experience utilizing the data in actual calculations. Although the amber PET used in the evaluation of the IR absorption was rather opaque, it is seen from Figure 43 that the % IR transmission for Shell material is much lower than that for amber PET. In order to obtain a more reliable IR heating characteristic of the material, the IR absorption coefficients should be evaluated using a thicker (3-4 mm) specimen.

8.0 Injection Blow Molding

8.1 Introduction

The new proprietary materials, 89022 and 89046, have successfully been processed by means of injection molding, thermoforming, and extrusion blow molding by Shell Engineering. However, these processes have failed to make a clear container. In order to make a clear container, an orientation process is necessary. As a result, it is thought that the Nissei injection stretch blow molding process might be successful in establishing the necessary orientation that is required to produce a clear container.

The Polymer Institute, in conjunction with Shell technical personnel, visited the Nissei Plant, Atlanta, Georgia, on July 25-26, and again on August 28-29, 1990. The purpose of these visits was to make clear, oriented bottles, using Shell Proprietary Resins on a Nissei Injection-blow molding machine.

8.2 Experimental

The Nissei ASB 50HT No. 8505134 injection stretch blow molding machine was used in the trials. The machine contained a hopper, screw, and four rotational stations which were used for injection molding, temperature conditioning, stretch blow molding, and releasing.

The dried Shell resins were injected molded into preforms on station #1. Preforms then were moved to station #2 to be temperature equilibrated. The inside of the preform was heated by a heater rod controlled by voltage, and outside the preform, temperature was controlled by contact with the mold cavity containing two temperature zones, controlled by thermolators. After the temperature conditioning, the preform was transferred to station #3 for blow molding, followed by stripping on station #4.

Shell materials used were 89021, 89045, 89046 (89022 was not available).

8.3 Conclusions

- The material 89021 proved to be too unstable and subject to degradation during blow molding trials.
- The materials 89045 and 89046 were less subject to degradation and bottles were made from 89045. The processing operating window proved to be quite narrow, and the inside of the bottle delaminated for unknown reasons.

8.4 Results and Discussion

Visit #1 (July 25-26, 1990), the initial trial, was semi-successful. Three materials were evaluated, 89021, 89045, and 89046. The major problem was material degradation. The injection barrel temperatures for processing 89045 are shown below.

Run #	Zone 1 (°C)	Zone 2 (°C)	Zone 3 (°C)
1	235	240	245
2	245	255	260
3	235	240	240
4	275	260	240

The result of processing 89046 for each run was the same, material degradation.

Material 89021, which was processed with the conditions of Run #4, also showed degradation.

For blow molding, the 89045 parisons from Run #4 were blow molded into 8 oz., 12 oz., and 16 oz. round bottles from the parison shown in Figure 45. Each of the temperature profiles, for blow molding, are shown below.

Run #	Zone 1 (°F)	Zone 2 (°F)
1	365	365
2	375	315
3	380	380
4	385	385
5	390	390
6	400	400

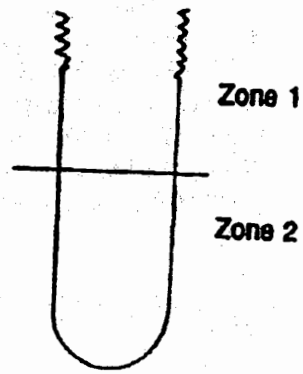

The result was hazy bottles, which may be the result of material degradation and insufficient orientation.

Figure 45 **Parison used on Nissei Visit #1**

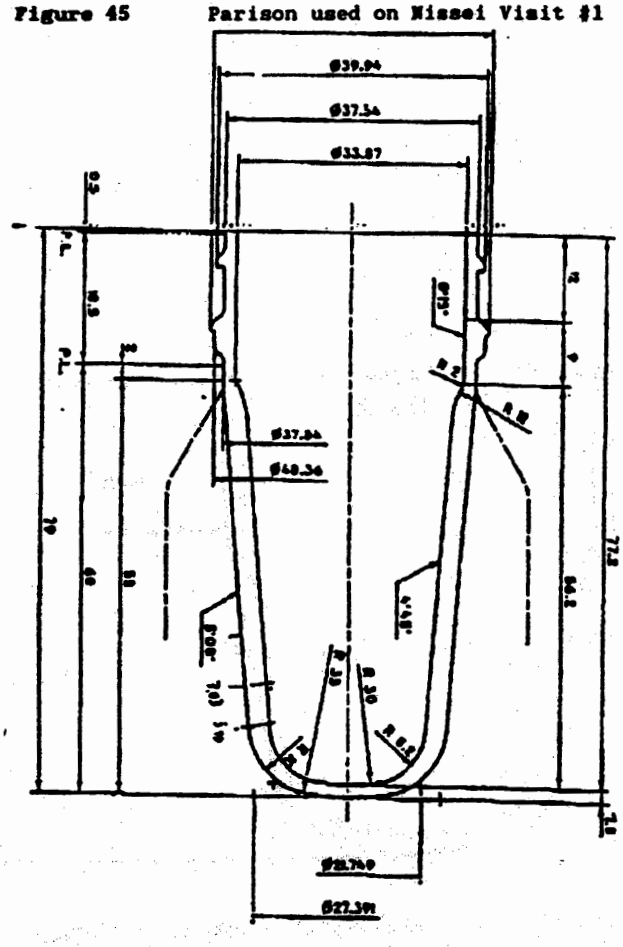

Visit #2 to Nissei occurred on August 28-29, 1990. The purpose was to reevaluate 89045 material.

The processing conditions were as follows:

Injection Barrel:	Zone 1	240°C
	Zone 2	260°C
	Zone 3	255°C
Conditioning Station:	Zone 1	410°F
	Zone 2	400°F

Figure 46 Parison used on Nissei Visit #2

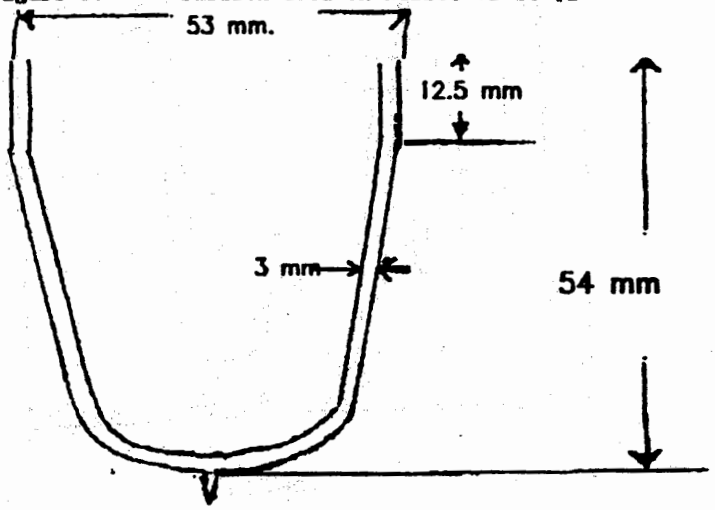

The parison used for visit #2 is shown in Figure 46. The 89045 material was stable during the two day trial. Only slight degradation was observed, and bottle clarity was better than visit #1. However, bottles were yellow in color and gels were visible.